Combined Large-Scale Phenotyping and Transcriptomics in Maize Reveals a Robust Growth Regulatory Network[1][OPEN]

Joke Baute, Dorota Herman, Frederik Coppens, Jolien De Block, Bram Slabbinck, Matteo Dell'Acqua, Mario Enrico Pè, Steven Maere, Hilde Nelissen, and Dirk Inzé*

Department of Plant Systems Biology, Vlaams Instituut voor Biotechnologie, 9052 Ghent, Belgium (J.B., D.H., F.C., J.D.B., B.S., S.M., H.N., D.I.); Department of Plant Biotechnology and Bioinformatics, Ghent University, 9052 Ghent, Belgium (J.B., D.H., F.C., J.D.B., B.S., S.M., H.N., D.I.); and Institute of Life Sciences, Scuola Superiore Sant'Anna, 56127 Pisa, Italy (M.D., M.E.P.)

ORCID IDs: 0000-0003-0507-6904 (J.B.); 0000-0001-6565-5145 (F.C.); 0000-0003-0047-4380 (J.D.B.); 0000-0002-4961-6231 (M.D.); 0000-0002-5341-136X (S.M.); 0000-0001-7494-1290 (H.N.); 0000-0002-3217-8407 (D.I.).

Leaves are vital organs for biomass and seed production because of their role in the generation of metabolic energy and organic compounds. A better understanding of the molecular networks underlying leaf development is crucial to sustain global requirements for food and renewable energy. Here, we combined transcriptome profiling of proliferative leaf tissue with in-depth phenotyping of the fourth leaf at later stages of development in 197 recombinant inbred lines of two different maize (*Zea mays*) populations. Previously, correlation analysis in a classical biparental mapping population identified 1,740 genes correlated with at least one of 14 traits. Here, we extended these results with data from a multiparent advanced generation intercross population. As expected, the phenotypic variability was found to be larger in the latter population than in the biparental population, although general conclusions on the correlations among the traits are comparable. Data integration from the two diverse populations allowed us to identify a set of 226 genes that are robustly associated with diverse leaf traits. This set of genes is enriched for transcriptional regulators and genes involved in protein synthesis and cell wall metabolism. In order to investigate the molecular network context of the candidate gene set, we integrated our data with publicly available functional genomics data and identified a growth regulatory network of 185 genes. Our results illustrate the power of combining in-depth phenotyping with transcriptomics in mapping populations to dissect the genetic control of complex traits and present a set of candidate genes for use in biomass improvement.

In plants, leaves are the main organs for fundamental biological functions, such as photosynthesis and respiration. The size, shape, and number of leaves strongly determine a plant's photosynthetic capacity and the efficiency with which water and nutrients are used. Consequently, the size of the leaves influences plant biomass and yield (Linkies et al., 2010; Pérez-Pérez et al., 2010). Therefore, understanding the mechanisms controlling various aspects of leaf development, such as growth rate and final size, is of great interest, in particular since the demands in food, feed, and renewable bioenergy are envisaged to increase strongly in the next decades (Godfray et al., 2010).

Leaf size is a complex trait determined by the interplay of several factors. The dynamics of leaf development have been studied in detail in various plant species at the organ and cellular levels, but insight into the underlying molecular mechanisms remains limited. Typically, leaf development starts with the recruitment of founder cells at the peripheral zone of the shoot apical meristem, followed by a phase of cell proliferation and successive cell expansion. During this postprimordial development, leaf differentiation progresses basipetally in monocots: the region containing proliferating cells becomes gradually restricted to the base of the organ; as a consequence, a growing leaf shows a developmental gradient with dividing cells at the base, fully differentiated mature cells at the tip, and in between a region of expanding cells (Poethig, 1984; Sylvester et al., 1990). At the molecular level, some genes that affect leaf size have been identified, primarily in the model species Arabidopsis (*Arabidopsis thaliana*; for review, see Gonzalez et al., 2012; Hepworth and Lenhard, 2014). Although regulators of both cell division and cell expansion have been identified, mutants or transgenic

lines with larger leaves tend to be composed of more cells rather than larger cells (Niklas, 1994; Gonzalez et al., 2010). For instance, leaves of maize (*Zea mays*) plants with altered levels of GA are affected in their growth rates, and the size of the division zone (DZ) is changed correspondingly (Nelissen et al., 2012). Examples in Arabidopsis of genes that are regulators of final leaf size by influencing cell proliferation are *AVP1*, *JAW*, and *BRI1* (Gonzalez et al., 2010), *GROWTH-REGULATING FACTOR1* (*GRF1*) and *GRF2* (Kim and Kende, 2004), *GRF5* (Horiguchi et al., 2005), *DA1* and *ENHANCER OF DA1* (Li et al., 2008), *ANGUSTIFOLIA3* (*AN3*)/*GRF-INTERACTING FACTOR* (Lee et al., 2009), and *KLUH* (Kazama et al., 2010). These examples illustrate that cell proliferation seems to be a key contributing factor to final leaf size.

Exploiting natural variation has been proposed as a complementary approach to the traditional, gene-centric reverse and forward genetics approaches to identify new genes (Weigel, 2012). Knockdown or overexpression of single genes does not capture the extensive genetic variation present in natural populations, which results from a combination of single-nucleotide substitutions, insertions, deletions, copy number variations, epigenetic changes, and expression differences. In the monocotyledonous species maize, the intraspecific variation is large and offers great potential to relate genotype to phenotype. Also, several mapping populations are available, but until now, only a few were used to determine the genetic control of leaf-related traits via quantitative trait locus (QTL) or genome-wide association studies (Pelleschi et al., 2006; Ku et al., 2010, 2012; Tian et al., 2011; Dignat et al., 2013). Although several small-effect QTLs were identified in these studies, further fine-mapping using complementary approaches or a priori knowledge is required to find the genes underlying the quantitative trait.

Previous studies found evidence that the phenotypic diversity in maize is mainly under transcriptional control (Li et al., 2012; Wallace et al., 2014). The recent availability of cost-efficient and high-throughput sequencing technologies to analyze transcriptomes provides new opportunities to gain further insights into the molecular basis of leaf size. In maize, several recent studies applied next-generation sequencing technologies to assess transcriptomic differences between leaf developmental stages and leaf cell types. Transcriptomes of different regions of a growing leaf, representing different developmental stages, were compared by Li et al. (2010) and Pick et al. (2011). Transcriptional dynamics during early development of embryonic leaves were surveyed by Liu et al. (2013b) and Yu et al. (2015). Additionally, the regulatory and functional differentiation of various leaf cell types was examined by transcriptome analysis (Li et al., 2010; Wang et al., 2013, 2014). The transcriptional variation between tissue types and cell types during development (Li et al., 2010; Wang et al., 2013, 2014) illustrates the importance of focusing the analysis of a given process on those tissues where the process takes place. Since leaf growth is driven by proliferation and expansion, zooming in on proliferative and/or expanding tissue is required to identify the regulatory networks underlying leaf development. The developmental gradient in growing maize leaves and the large size of the leaf makes it possible to dissect these specific growth zones for further analysis (Nelissen et al., 2012). Since it was recently suggested that it is the final number of cells that primarily determines final leaf size (Gonzalez et al., 2010; Nelissen et al., 2012), we focus our transcriptome analysis specifically on proliferative tissue of the growing leaf.

Although analyses of transcriptional variation during maize leaf development have provided us with new insights, all these studies were restricted to one genetic background (Li et al., 2010; Pick et al., 2011; Liu et al., 2013b; Wang et al., 2013, 2014; Yu et al., 2015). Adding an additional layer of information, phenotypic variation in mapping populations, and combining this with transcriptome variation in these populations offers new opportunities to identify genes and regulatory mechanisms that are at the basis of phenotypic differences (Andorf et al., 2012).

Recently, we associated phenotypic variation with transcriptome variation in 103 lines of a biparental recombinant inbred line (RIL) population (Baute et al., 2015). We described the relationship of leaf size traits, such as final leaf area and leaf weight, and transcriptional variation in fully proliferative tissue sampled during early leaf development. Although the genetic and phenotypic variation in a classical biparental RIL mapping population provides a valuable source of information, the possibility to detect variation in expression that is associated with phenotypic variation remains limited, since it depends on the polymorphisms between only two parents. In multiparent advanced generation intercross (MAGIC) populations, RILs are generated from multiple parents by mixing the genomes of the founder lines through several rounds of mating, followed by inbreeding to obtain a set of stable homozygous lines (Churchill et al., 2004; Cavanagh et al., 2008; Kover et al., 2009). Such a MAGIC population was recently established for maize, and a panel of 529 lines was genotyped (Dell'Acqua et al., 2015). The population has a larger genetic diversity than biparental populations, and as such, the number of components in the regulatory network that can be identified is expected to be higher. Moreover, integrating results from different populations may allow for the identification of the most robust players in the growth-related molecular network across different lines. In this study, we performed detailed phenotyping and transcriptome analysis of 94 lines of the MAGIC population and combined this with the previously described phenotyping and transcriptome analysis of 103 lines of the biparental B73 × H99 population. We identified a set of 226 genes with expression levels in the DZ of the growing leaf (anti)correlating with leaf phenotype measurements in both populations. Some of these

genes have homologs in Arabidopsis with a known function in leaf development. However, the majority of the genes had no known function or were not annotated before as having a role in this process, implying that these might be interesting candidates to further decipher the molecular network underlying leaf development. Additionally, integration of publicly available functional genomics data (De Bodt et al., 2012) led to the identification of a subset of 185 genes that are interconnected through expression correlations or protein-protein interactions.

RESULTS AND DISCUSSION

Correlation between Leaf Size and Shoot Traits Is Similar in the Two Different Populations

Previously, in-depth phenotyping of 103 lines of a biparental RIL population derived from the inbred parents B73 and H99 (Marino et al., 2009) was combined with transcriptome profiling to dissect leaf size, growth, and shoot-related traits into phenotypic and molecular components (Baute et al., 2015). Here, a similar analysis was conducted on the recently

established multiparent MAGIC population (Dell'Acqua et al., 2015), and results of both analyses were integrated. Concerning phenotyping, final leaf size-related traits, such as leaf length (LL), leaf width (Lwi), leaf area (LA), and leaf weight (Lwe), were complemented with measurements that capture growth kinetics, such as growth rate (leaf elongation rate [LER]) and duration (emergence, time point of maximal LER [Tm], time point when leaf 4 reaches its final length [Te], and leaf elongation duration [LED5-e]; Voorend et al., 2014), and cellular measurements, such as the size of the cell DZ. In addition, whole-shoot variables were measured at the seedling stage: fresh weight, dry weight, leaf number (LN), and vegetative (V)-stage (maize leaf stage; Baute et al., 2015; Fig. 1; Supplemental Table S1).

Pearson correlation coefficients (PCCs) between the traits were determined based on the data obtained for the MAGIC population (Table I), for the combined data of both populations (Supplemental Table S2), and compared with our previous analysis for the biparental RIL population (Table I; Baute et al., 2015). All three analyses gave comparable results and supported the separation of the traits into three groups: leaf size traits (LL, Lwe, LA, Lwi, LER, and DZ size), shoot-related
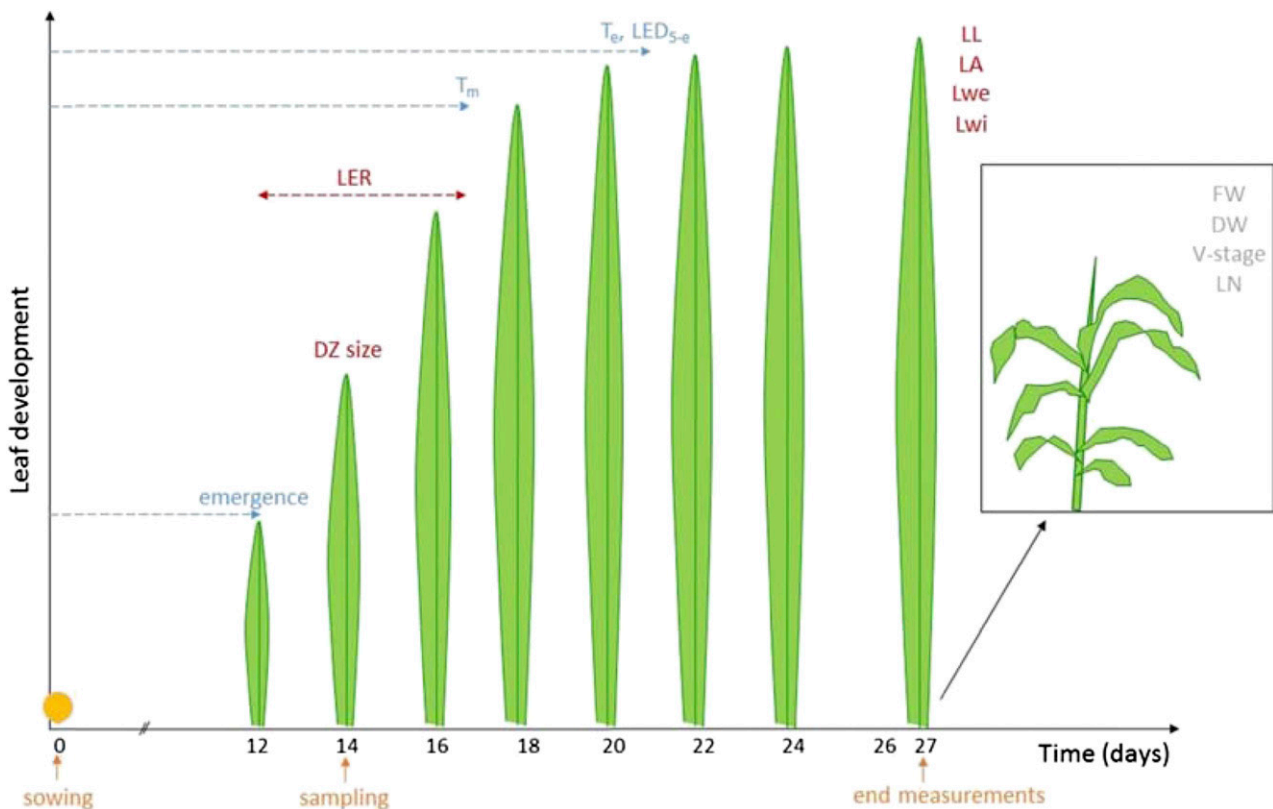
Figure 1. Schematic representation of maize leaf development as a function of time and phenotyping strategy. Shown is the leaf growth of B73. LL was measured daily from emergence from the surrounding leaves until 27 d after sowing. LER, T_m, T_e, and LED_{5-e} were deduced from these daily measurements. DZ size was determined 2 d after leaf emergence, at the same time that leaf material was sampled for RNA sequencing. End measurements, LL, LA, Lwe, Lwi, fresh weight (FW), dry weight (DW), V-stage, and LN, were determined 27 d after sowing, when leaf 4 had reached its mature size for all RILs.

Table I. *PCC for the analyzed traits, grouped as leaf size, shoot-related, and timing-related traits for biparental and MAGIC RIL populations*

Significant correlations are indicated by asterisks (**, $P < 0.01$ and *, $P < 0.05$); highly significant positive correlations are indicated in italics, and highly significant negative correlations are indicated in bold.

Biparental RIL Population (Bottom Diagonal)	MAGIC RIL Population (Top Diagonal)													
	LER	LL	Lwe	LA	Lwi	DZ Size	Fresh Weight	Dry Weight	LN	V-Stage	Emergence	T_e	T_m	LED_{5-e}
LER		0.772**	0.517**	0.466**	0.151	0.347**	0.607**	0.658**	0.187	0.081	−0.069	−0.082	−0.054	−0.045
LL	0.738**		0.775**	0.782**	0.487**	0.615**	0.355**	0.427**	−0.259*	−0.435**	0.239*	0.421**	0.387**	0.502**
Lwe	0.493**	0.750**		0.904**	0.787**	0.562**	0.418**	0.419**	−0.286**	−0.500**	0.338**	0.496**	0.461**	0.556**
LA	0.479**	0.781**	0.915**		0.880**	0.603**	0.289**	0.356**	−0.354**	−0.585**	0.399**	0.585**	0.528**	0.660**
Lwi	0.063	0.316**	0.688**	0.794**		0.478**	0.102	0.14	−0.435**	−0.623**	0.475**	0.616**	0.565**	0.659**
DZ size	0.507**	0.594**	0.516**	0.526**	0.308**		0.279**	0.315**	−0.137	−0.301**	0.142	0.320**	0.248*	0.423**
Fresh weight	0.520**	0.215*	0.413**	0.297**	0.17	0.211*		0.939**	0.614**	0.456**	−0.473**	−0.455**	−0.481**	−0.342*
Dry weight	0.502**	0.206*	0.311**	0.245*	0.098	0.219*	0.893**		0.601**	0.414**	−0.499**	−0.433*	−0.476**	−0.297*
LN	0.176	−0.255	−0.258	−0.273	−0.267	−0.251	0.521**	0.377*		0.834**	−0.735**	−0.816**	−0.818**	−0.752**
V-stage	0.083	−0.423**	−0.420**	−0.472**	−0.375*	−0.266	0.435**	0.326*	0.834**		−0.725**	−0.887**	−0.866**	−0.860**
Emergence	0.007	0.245*	0.258*	0.291**	0.307**	0.097	−0.455**	−0.462**	−0.649**	−0.599**		0.865**	0.911**	0.742**
T_e	−0.105	0.379**	0.328*	0.414**	0.365**	0.113	−0.582**	−0.557**	−0.621**	−0.701**	0.620**		0.976**	0.960**
T_m	−0.048	0.374**	0.334*	0.413**	0.379**	0.118	−0.568**	−0.557**	−0.601**	−0.675**	0.650**	0.979**		0.880**
LED_{5-e}	−0.114	0.424**	0.332*	0.418**	0.298**	0.147	−0.470**	−0.420**	−0.568**	−0.656**	0.461**	0.894**	0.787**	

traits (fresh weight, dry weight, LN, and V-stage), and timing-related traits (emergence, T_m, T_e, and LED_{5-e}; Table I; Supplemental Table S2; Supplemental Fig. S1). Also between groups of traits, the correlations were largely the same in the two populations.

In general, the PCCs were higher for the MAGIC population than for the biparental RIL population, especially among leaf, shoot, and timing traits and between leaf-shoot and leaf-timing traits, which may be due to the fact that the phenotype variation in the MAGIC population is generally larger than that of the biparental RIL population (i.e. the phenotype distributions are broader; Supplemental Table S1; Supplemental Fig. S2), which may suppress the negative influence of stochastic and measurement noise on PCC values. A larger phenotypic variation in the eight-way RIL population was expected, given the increased variation in the phenotypes of the parents compared with the biparental mapping population (Supplemental Fig. S2). As an exception, the PCC between LER and DZ size was lower in the MAGIC population than in the biparental population, 0.347 and 0.507, respectively. Also, the anticorrelations between the timing traits and shoot traits fresh weight and dry weight were slightly stronger in the biparental population than in the MAGIC population (Table I). Possibly, the biparental population already covers a large part of the variability for the timing and shoot

traits, while additional power is available in the MAGIC population for the leaf size traits. This is confirmed if we determine the positions of the parental lines in the distributions of the two populations (Supplemental Fig. S2): for the leaf size traits LL, Lwe, LA, and Lwi, values for the parental lines B73 and H99 are very similar, while they are more diverse for the other traits.

Correlation between Traits Is Fully Supported at the Transcriptome Level

In both populations, DZ size correlated positively with the leaf size traits and, to some extent, with shoot fresh weight and dry weight (Table I; Supplemental Table S2; Supplemental Fig. S2). This supports the hypothesis that the number of dividing cells is one of the key factors in the determination of final organ size and that the transcriptional differences between genotypes in proliferative tissue may inform us on important players that determine final size traits. We previously performed RNA sequencing of proliferative leaf tissue of 103 lines of the biparental RIL population (Baute et al., 2015) and extended this here with RNA sequencing of comparable tissue of 94 lines of the MAGIC population.

Linear correlation between phenotypes and transcript levels was determined by calculating PCCs between the expression level of each transcript and each trait in both populations separately. The $q_{0.99}$ and $q_{0.01}$ PCC (i.e. the correlation coefficient of the 1% best [anti] correlating transcripts) were determined before and after permutation of the trait data (for details, see "Materials and Methods"). For the majority of the traits, the $q_{0.99}$ and $q_{0.01}$ PCC values were significantly higher than those expected at random (Fig. 2), indicating that the gene sets identified by this arbitrarily chosen limit of 1% contain genes whose expression levels in proliferative tissue of a growing leaf correlate significantly with final size measurements. For the leaf size traits in particular, the $q_{0.99}$ and $q_{0.01}$ PCC were higher in the MAGIC population than in the biparental RIL population. As the cutoffs defined by permuting the data were very comparable for both populations (Fig. 2), this resulted in a higher number of genes with a PCC greater than the $q_{0.99,random}$ PCC in the MAGIC population (Table II), indicating that the higher variability in the MAGIC population facilitates the identification of significant transcript-phenotype correlations for leaf size traits. On the other hand, $q_{0.99}$ and $q_{0.01}$ PCC for fresh weight and dry weight were considerably lower in the MAGIC population than in the biparental RIL population, suggesting that the relationship between gene expression and fresh weight and dry weight traits in the eight-way population may be more complex and nonlinear in nature than in the two-way population, due to an increased number of different alleles that play a role. Accordingly, the number of genes with a PCC higher than the $q_{0.99,random}$ PCC or lower than the $q_{0.01,random}$ PCC for dry weight and fresh weight in the MAGIC population was lower than in the biparental

population, and the number of genes in the intersection of both populations was limited and not higher than expected by chance (Table II). Also for LER, the percentage of genes found in common for the two populations was small and not higher than expected by chance ($P > 0.05$), while for all other traits, the overlap was significant (Table II). In both populations, the $q_{0.99}$ and $q_{0.01}$ PCC for LER were lower than for the other traits (Fig. 2). The lack in significant overlap between the two populations of transcripts whose expression correlated to LER, fresh weight, and dry weight indicates that another range of growth mechanisms and networks may be active and/or captured for these three traits in the different populations.

Further analyses were restricted to the 1% best correlating and anticorrelating genes for each trait, or 286 genes for each trait, referred to below as the correlated and anticorrelated gene sets. Importantly, although some traits had $q_{0.99}$ and $q_{0.01}$ PCC close to the corresponding q_{random} PCC, in all cases the selected 286 genes had a PCC higher or lower than the $q_{0.99}$ and $q_{0.01}$ thresholds, respectively, and thus higher or lower than the corresponding q_{random} PCC. The total number of genes thus selected for at least one trait was 22% lower in the MAGIC population (1,367) than in the biparental RIL population (1,740), since the gene selection for the MAGIC population contains a higher proportion of genes that correlate with several traits compared with the biparental RIL population (Fig. 3A). This might be due to the higher correlation between the leaf size traits in the MAGIC population. In the MAGIC population, we found 21 genes (Supplemental Table S3) associated with nine traits, the maximum in the biparental RIL population being eight traits. One of these 21 genes, *GRMZM2G389768*, with homology to cold shock

Figure 2. The 0.99 and 0.01 quantiles of distribution of Pearson correlation between transcript expression levels and traits. Real data are shown in dark gray (biparental RIL population) and light gray (MAGIC RIL population) bars; permuted data are shown in dark gray (biparental RIL population) and light gray (MAGIC RIL population) lines. Error bars indicate SD of the permuted data ($n = 1,000$) in dark gray for the biparental population and in light gray for the MAGIC population. DW, Dry weight; FW, fresh weight.
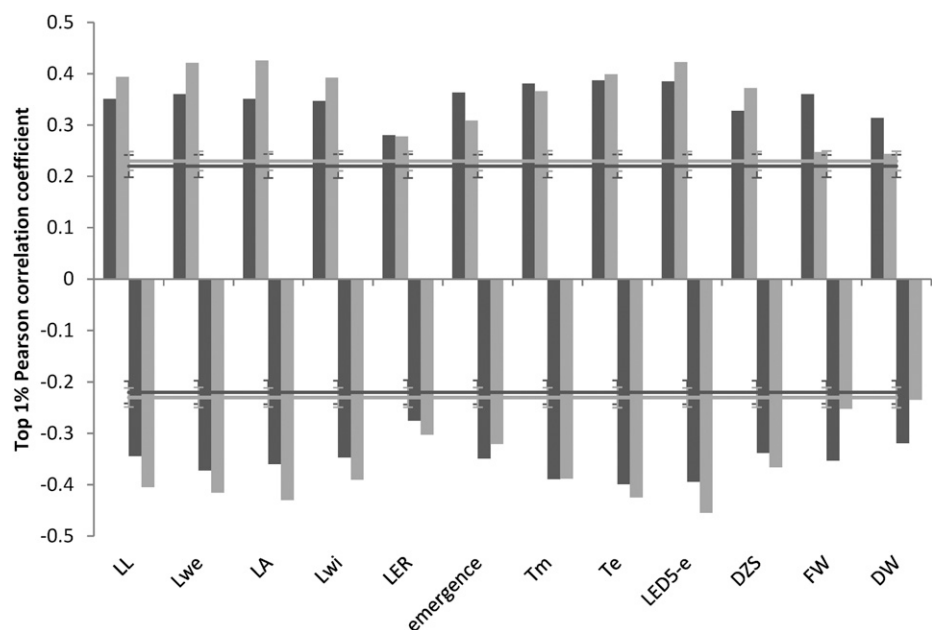
Table II. *Number of genes correlating with traits in biparental and MAGIC RIL populations, and number and percentage of genes in the intersections*

Significance is designated as follows: *, significantly enriched ($P < 0.05$); NS, not significant ($P > 0.05$), according to hypergeometric probability testing.

Trait	Correlation (Random)[a]			Significance	Correlation (Quantiles)[b]			Significance
	Biparental	MAGIC	Intersection		Biparental	MAGIC	Intersection	
LL	2,206	3,111	740 (34%)	*	286	286	51 (18%)	*
Lwe	2,596	3,141	928 (36%)	*	286	286	54 (19%)	*
LA	2,230	3,165	1,039 (47%)	*	286	286	71 (25%)	*
Lwi	2,477	2,504	789 (32%)	*	286	286	30 (10%)	*
LER	1,073	1,174	70 (7%)	NS	286	286	6 (2%)	NS
DZ size	1,927	2,228	765 (40%)	*	286	286	82 (29%)	*
Emergence	2,490	1,463	436 (30%)	*	286	286	25 (9%)	*
T_m	3,171	2,368	903 (38%)	*	286	286	24 (8%)	*
T_e	3,260	2,892	1,202 (42%)	*	286	286	34 (12%)	*
$LED_{5\text{-}e}$	3,003	3,419	1,335 (44%)	*	286	286	58 (20%)	*
Fresh weight	2,259	530	77 (15%)	NS	286	286	4 (1%)	NS
Dry weight	1,707	401	56 (14%)	NS	286	286	5 (2%)	NS

[a]Numbers of genes with PCC greater than q_{random} PCC.   [b]Genes in $q_{0.01}$ and $q_{0.99}$ in the intersection of two data sets.

domain proteins, correlated with eight traits in the biparental RIL population. In both populations, the numbers of (anti)correlating genes shared between traits was higher within the three trait groups (leaf size, timing, and shoot) than between these groups (Fig. 3, B and C), in accordance with the correlations found at the phenotype level. As for the biparental population (Baute et al., 2015), no opposite gene-trait correlations with traits that were categorized in the same group were found for the MAGIC population (numbers in blue in Fig. 3, B and C). Opposite correlation of a transcript with multiple traits was very limited in both populations, 84 and 28 genes in the two-way and eight-way populations, respectively, and was observed only for timing-related traits versus shoot-related traits, traits that are also anticorrelated at the phenotype level.

Combining the Two Populations Identifies Genes That Are Robustly Associated with the Traits

In the separate populations, expression levels of 1,740 and 1,367 genes in the biparental and MAGIC populations, respectively, correlated with at least one of the traits. Of these genes, 226 were (anti)correlating with at least one of the traits in both populations, a strong reduction compared with the numbers found in the populations separately (Supplemental Table S3). The expression levels of the 226 (anti)correlating genes in all RILs and their association with the traits were visualized in a clustered heat map (Fig. 4), revealing a clear gradient in expression levels that were coinciding with (Fig. 4A) or opposite to (Fig. 4B) the phenotypic variation observed in the RILs. The 226 genes in common for both populations were unevenly distributed over the different traits. The percentage of (anti)correlating genes in the quantiles that was shared between the two populations ranged from a few percent for LER, fresh weight, and dry weight up to 29% for

DZ size (Table II). For all traits except LER, fresh weight, and dry weight, the number of genes in the intersection was larger than expected by chance (hypergeometric test; $P < 0.05$), and overall, the number of genes in the intersection was highest for leaf size traits. It is worth noting that for none of the traits were there correlating genes in one population and anticorrelating genes in the other population. The strong reduction of the number of correlated genes by combining the two populations, combined with the fact that the overlap remains significantly higher than expected by chance for the majority of the traits, indicates that this approach is efficient in identifying the genes that are more robustly associated with a specific trait, regardless of the population context, and thus might be more relevant to characterize functionally.

Enriched Functional Categories Are Partially Overlapping for the Two Populations

All genes were assigned to MapMan functional categories (Thimm et al., 2004), and tests for the enrichment of functional categories in the correlating gene sets for the different traits were performed for the two populations separately, to verify if gene sets were enriched for comparable categories in the two populations (Supplemental Fig. S3). For positively correlating genes, the major enriched functional category in both populations was regulation of transcription. The functional categories hormone metabolism, protein modifications, and protein degradation were enriched for several traits in the biparental RIL population but not or for only one trait in the MAGIC population. Regulation of transcription, protein synthesis, and cell wall synthesis and degradation were significantly enriched categories for the negatively correlated gene sets for multiple traits in both populations. Thus, the major enriched functional categories are regulation of transcription, protein synthesis, and cell wall synthesis

Figure 3. Number of genes correlating with one or multiple traits. A, Percentage of genes (anti)correlating with the traits in the biparental RIL population (dark gray) and the MAGIC population (light gray). B and C, Venn diagrams of the number of genes correlating (numbers in red), anticorrelating (numbers in green), or both (numbers in blue) with at least one of the leaf size, shoot, and timing traits in the biparental RIL population (B) and the MAGIC population (C).
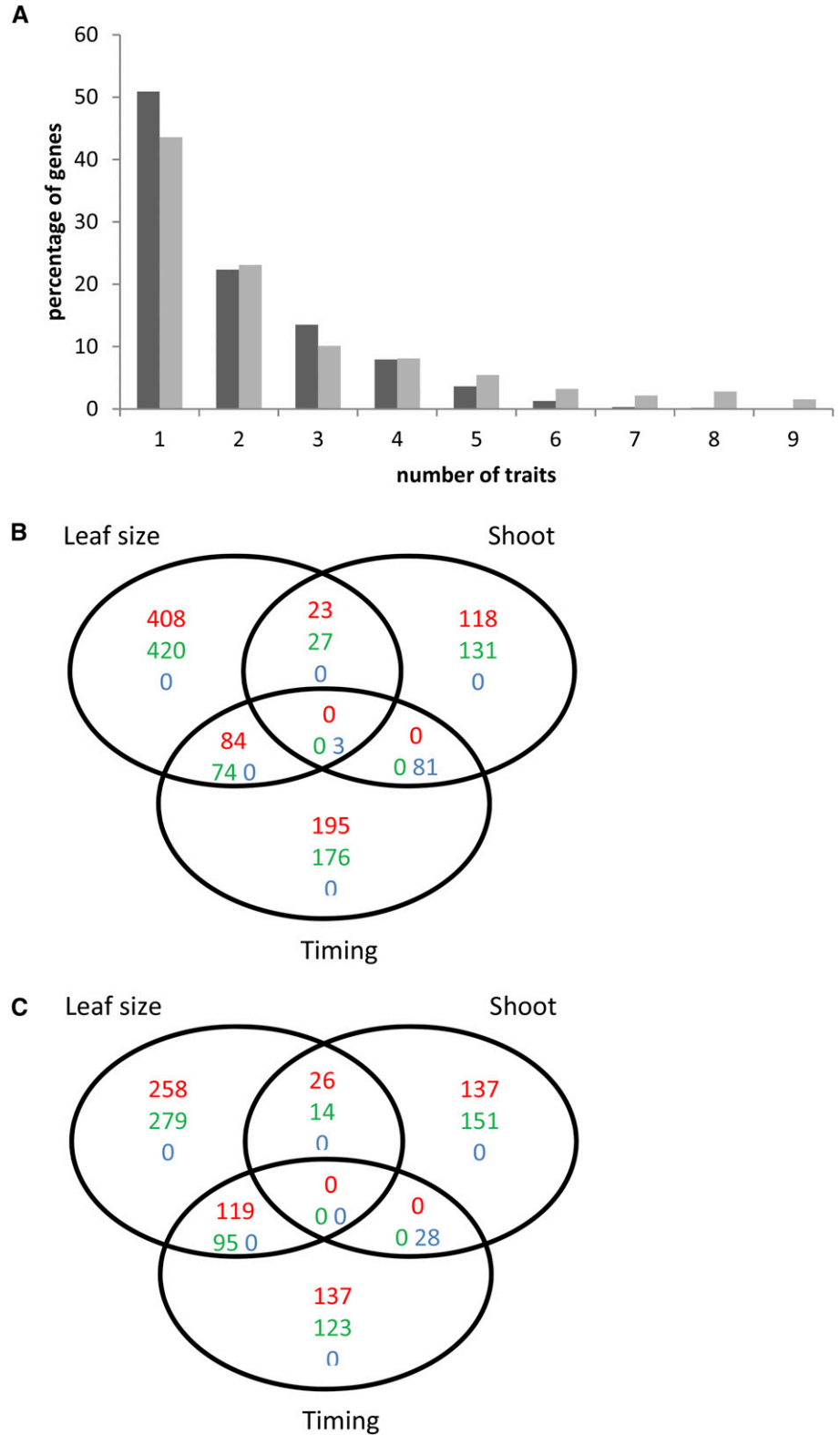
and degradation, with 56, 28, and 15 genes in common between the two populations.

Next, we compared the frequencies of all functional categories in the intersection of both populations

(i.e. the 226 genes) with their frequencies in the populations independently (i.e. the 1,740 and 1,367 genes in the biparental and MAGIC populations, respectively) to try to understand the nature of processes conserved
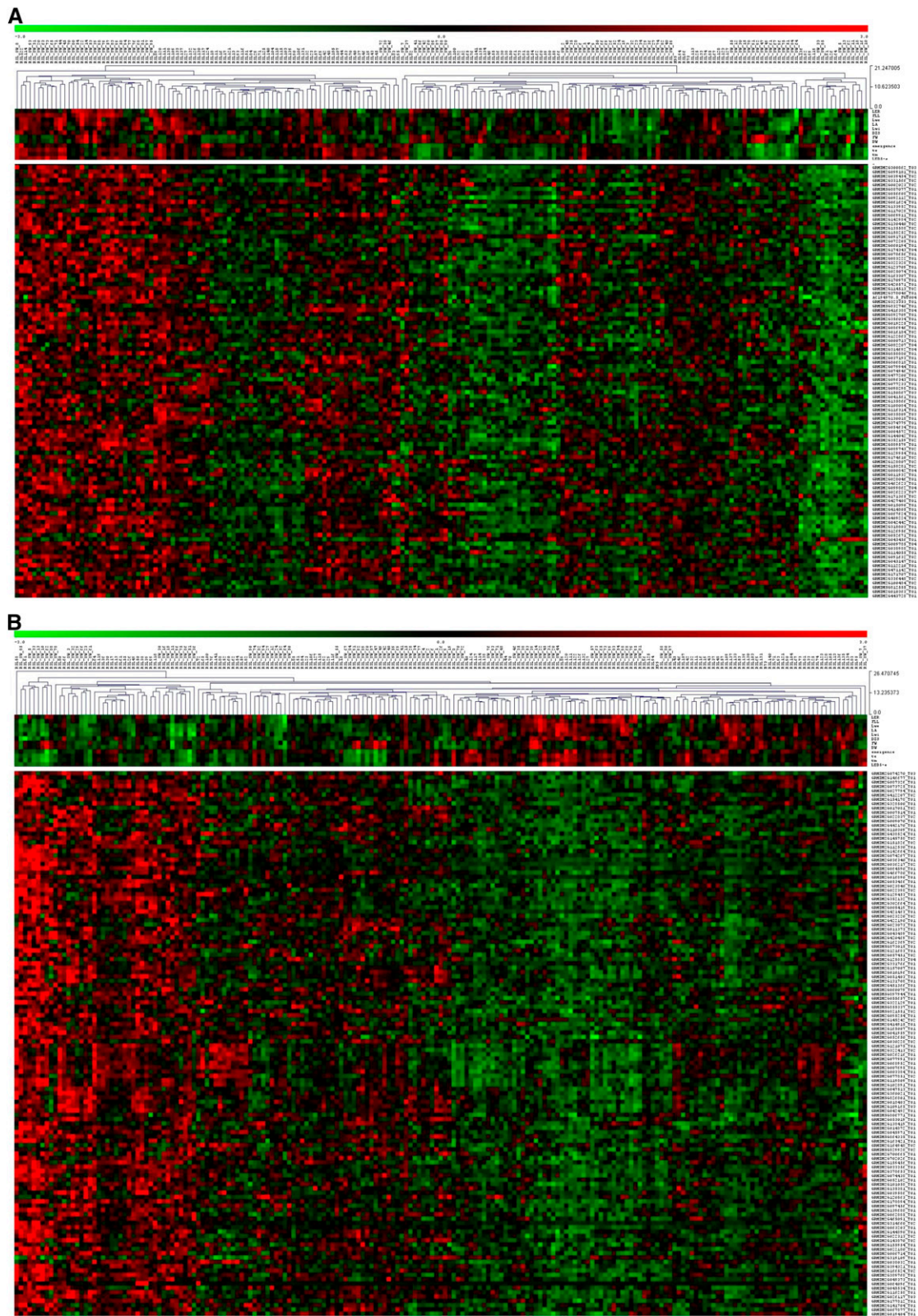
Figure 4. Expression levels of the 226 correlating and anticorrelating genes in all RILs. A, Correlated genes. B, Anticorrelated genes. Columns represent RILs of the two populations that were hierarchically clustered, and rows represent gene expression profiles with, on top, above the white separation, a heat map of the phenotypic traits. Green indicates low values and red indicates high values.

across the two populations. The functional categories regulation of transcription, protein synthesis, and cell wall synthesis and degradation were significantly ($P <$ 0.05) enriched 1.8-, 3-, and 2.5-fold, respectively, in the intersection compared with the complete gene set correlated with the biparental population, while compared with the MAGIC population, the two functional categories regulation of transcription and cell wall synthesis and degradation were enriched significantly ($P < 0.05$) 1.4- and 1.8-fold, respectively. This underscores the usefulness of focusing on the intersection for identifying the processes conserved in different populations, since largely the same processes are enriched in both analyses.

The three major functional categories we identified, regulation of transcription, protein synthesis, and cell wall synthesis and degradation, are described in more detail in the following sections.

Transcription Factors Involved in Hormone Regulation, Leaf Architecture Traits, and Chromatin Structure Correlate Robustly with Leaf Size

To obtain a better understanding of the nature of the regulatory processes during leaf growth, we focused on the 56 transcription factor (TF) genes whose expression levels were correlating with traits in both populations. Breakdown of the functional category regulation of transcription into the different TF families revealed that the major classes of TFs in the gene sets that are positively correlated with the traits are *ARGONAUTE, MADS* box, *SQUAMOSA PROMOTER-BINDING PROTEIN* (*SBP*), *SET, GRF,* and *bZIP,* while the major classes of TFs that are negatively correlated with the traits are *bHLH, GATA,* and *TRIHELIX* (Fig. 4). As determined with the Bio-Analytic Resource for maize gene expression (http://bar.utoronto.ca/efp_maize), about one-third of these TFs are expressed specifically in the DZ (Fig. 5). This is less than expected, since, according to Li et al. (2010), approximately 70% of all TFs show DZ-specific expression. Among the 56 TFs, we could identify 22 reported before to be linked to growth (Fig. 5). Many of these are related to hormone signaling, leaf architecture, and chromatine structure, three classes that are discussed in more detail below.
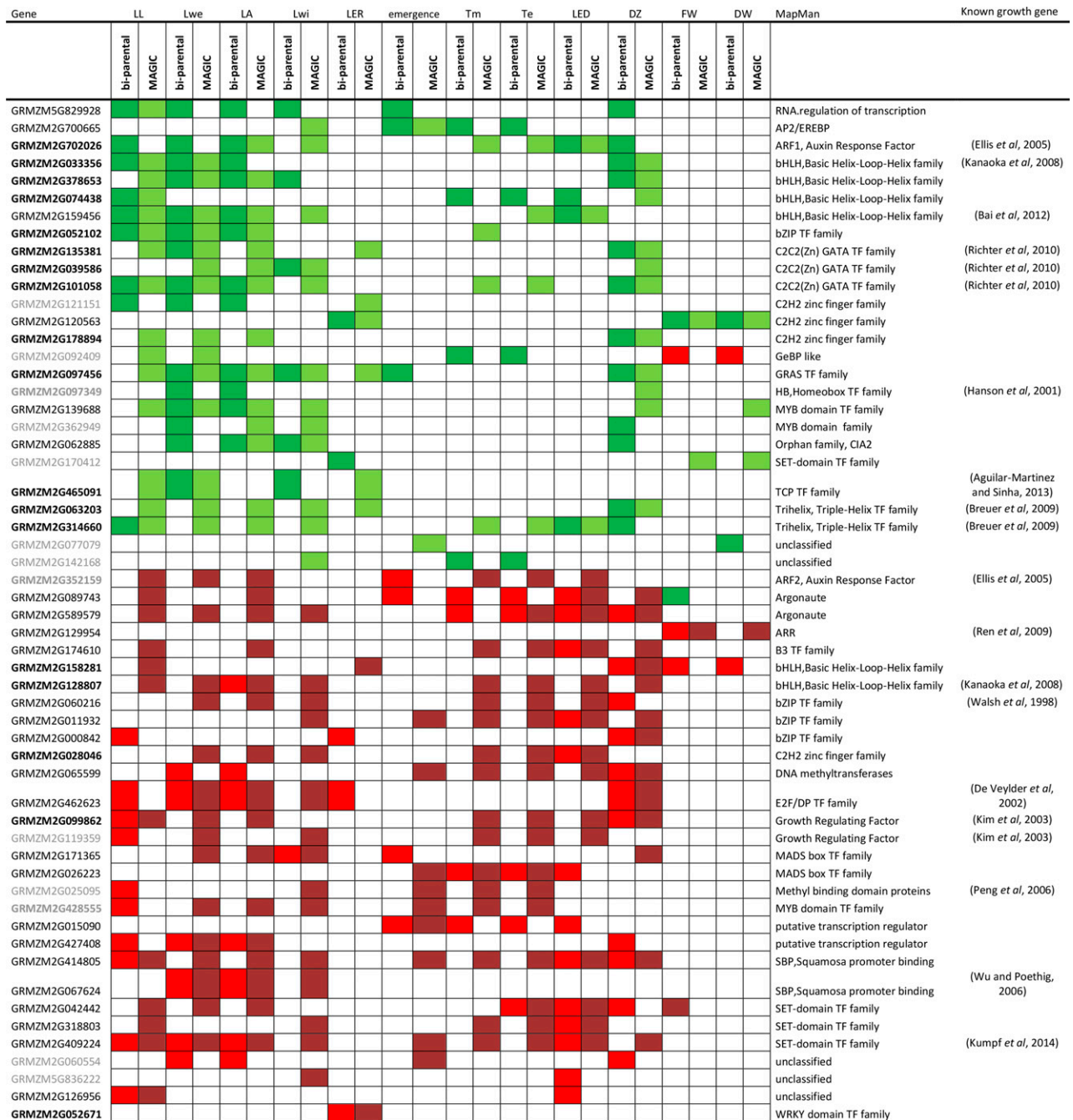
Our data set contains three GATA-type TFs that show a negative correlation with the leaf size-related traits (Fig. 5). In Arabidopsis, two redundant GATA-type TFs, *GATA, NITRATE-INDUCIBLE, CARBON-METABOLISM INVOLVED* (*GNC*) and *GNC-LIKE/ CYTOKININ-RESPONSIVE GATA FACTOR1* (*GNL/ CGA1*), were identified to regulate multiple aspects of plant development by repressing GA signaling. In agreement with the anticorrelation between the transcript level and leaf size, double mutants displayed increased rosette sizes, while overexpression resulted in smaller plants (Richter et al., 2010). Moreover, it was shown that these GATA factors act downstream of *AUXIN RESPONSE FACTOR2* (*ARF2*), which was also

identified in the subset of 56 TFs. *GNC* and *GNL* overexpressors show phenotypic similarities with *arf2* mutants (Richter et al., 2013). In agreement, *ARF2* expression levels were positively correlated with several traits (i.e. LL, Lwe, and LA), while expression levels of the GATA-type TFs were negatively correlated with these traits (Fig. 5). In addition, other TFs that are likely implicated in hormone regulation, such as *Arabidopsis Response Regulator* (*ARR,* cytokinin signaling; *GRMZM2G129954*; Ren et al., 2009) and *GRAS* (GA signaling; GRMZM2G097456) family members (Hirsch and Oldroyd, 2009), also correlated with the traits in both populations. A *bHLH* TF (*GRMZM2G159456*) with homology to the Arabidopsis and rice (*Oryza sativa*) paclobutrazol-resistant family of TFs, which mediate growth responses to multiple environmental and hormonal signals (Zhang et al., 2009; Bai et al., 2012), was negatively correlated with leaf size-related traits (Fig. 5).

Also correlated with leaf size traits were some TFs that are known to define leaf architecture traits. For example, the expression profile of LIGULELESS2 (LG2), a bZIP TF involved in establishing the position of the ligule (Walsh et al., 1998), was found to be positively correlated with leaf size- and timing-related traits (Fig. 5). Mutations in *LG2* affect leaf architecture due to a change in the leaf angle. However, no clear effect on leaf size has been reported (Tian et al., 2011), although *LG2* was mapped within a meta-QTL for leaf length and leaf width (Ku et al., 2012). Moreover, LG2 functions in the same pathway as LIGULELESS NARROW (LGN) and *lg2* transcripts are reduced in *lgn* mutants, which display a severe reduction in leaf size and total plant height (Moon et al., 2013).

As another example, the expression levels of two *SBP/SBP-LIKE* (*SPL*) genes, which regulate a wide variety of processes associated with shoot development, correlated with leaf size traits in our data set (Fig. 4): one maize-specific gene (*GRMZM2G414805*) and one gene (*GRMZM2G067624*) with homology to Arabidopsis *SPL4,* which is involved in vegetative phase change (Wu and Poethig, 2006). Another class of genes known to affect leaf architecture traits are the *TCP* TFs that contain a bHLH domain and are involved in the coordination of cell proliferation, cell differentiation, and growth; as such, they play a role in leaf development (Ori et al., 2007). One of the genes identified as correlated with leaf size traits, GRMZM2G465091, shows homology to Arabidopsis class I TCP proteins. Quadruple and pentuple loss-of-function mutants of class I *TCP* genes in Arabidopsis have larger but fewer rosette leaves (Aguilar-Martínez and Sinha, 2013), in agreement with the negative correlation between leaf size traits and expression levels of this maize homologous gene.

A third set of TFs that correlated with leaf size traits were related to chromatin structure. Three positively correlating SET domain TF family proteins were identified with homology to Arabidopsis SU(VAR)3-9 RELATED4 (SUVR4) and ASH1-RELATED3 (ASHR3),

Figure 5. TFs with expression profiles correlating or anticorrelating with at least one of the traits in both populations. Bright red indicates positive correlation in the biparental population, dark red indicates positive correlation in the MAGIC population, dark green indicates negative correlation in the biparental population, and light green indicates negative correlation in the MAGIC population. DZ-specific TFs are indicated in boldface (Li et al., 2010). DW, Dry weight; FW, fresh weight.

Gene	MapMan	Known growth gene
GRMZM5G829928	RNA.regulation of transcription	
GRMZM2G700665	AP2/EREBP	
GRMZM2G702026	ARF1, Auxin Response Factor	(Ellis et al., 2005)
GRMZM2G033356	bHLH,Basic Helix-Loop-Helix family	(Kanaoka et al., 2008)
GRMZM2G378653	bHLH,Basic Helix-Loop-Helix family	
GRMZM2G074438	bHLH,Basic Helix-Loop-Helix family	
GRMZM2G159456	bHLH,Basic Helix-Loop-Helix family	(Bai et al., 2012)
GRMZM2G052102	bZIP TF family	
GRMZM2G135381	C2C2(Zn) GATA TF family	(Richter et al., 2010)
GRMZM2G039586	C2C2(Zn) GATA TF family	(Richter et al., 2010)
GRMZM2G101058	C2C2(Zn) GATA TF family	(Richter et al., 2010)
GRMZM2G121151	C2H2 zinc finger family	
GRMZM2G120563	C2H2 zinc finger family	
GRMZM2G178894	C2H2 zinc finger family	
GRMZM2G092409	GeBP like	
GRMZM2G097456	GRAS TF family	
GRMZM2G097349	HB,Homeobox TF family	(Hanson et al., 2001)
GRMZM2G139688	MYB domain TF family	
GRMZM2G362949	MYB domain family	
GRMZM2G062885	Orphan family, CIA2	
GRMZM2G170412	SET-domain TF family	
GRMZM2G465091	TCP TF family	(Aguilar-Martinez and Sinha, 2013)
GRMZM2G063203	Trihelix, Triple-Helix TF family	(Breuer et al., 2009)
GRMZM2G314660	Trihelix, Triple-Helix TF family	(Breuer et al., 2009)
GRMZM2G077079	unclassified	
GRMZM2G142168	unclassified	
GRMZM2G352159	ARF2, Auxin Response Factor	(Ellis et al., 2005)
GRMZM2G089743	Argonaute	
GRMZM2G589579	Argonaute	
GRMZM2G129954	ARR	(Ren et al., 2009)
GRMZM2G174610	B3 TF family	
GRMZM2G158281	bHLH,Basic Helix-Loop-Helix family	
GRMZM2G128807	bHLH,Basic Helix-Loop-Helix family	(Kanaoka et al., 2008)
GRMZM2G060216	bZIP TF family	(Walsh et al, 1998)
GRMZM2G011932	bZIP TF family	
GRMZM2G000842	bZIP TF family	
GRMZM2G028046	C2H2 zinc finger family	
GRMZM2G065599	DNA methyltransferases	
GRMZM2G462623	E2F/DP TF family	(De Veylder et al, 2002)
GRMZM2G099862	Growth Regulating Factor	(Kim et al, 2003)
GRMZM2G119359	Growth Regulating Factor	(Kim et al, 2003)
GRMZM2G171365	MADS box TF family	
GRMZM2G026223	MADS box TF family	
GRMZM2G025095	Methyl binding domain proteins	(Peng et al, 2006)
GRMZM2G428555	MYB domain TF family	
GRMZM2G015090	putative transcription regulator	
GRMZM2G427408	putative transcription regulator	
GRMZM2G414805	SBP,Squamosa promoter binding	
GRMZM2G067624	SBP,Squamosa promoter binding	(Wu and Poethig, 2006)
GRMZM2G042442	SET-domain TF family	
GRMZM2G318803	SET-domain TF family	
GRMZM2G409224	SET-domain TF family	(Kumpf et al, 2014)
GRMZM2G060554	unclassified	
GRMZM5G836222	unclassified	
GRMZM2G126956	unclassified	
GRMZM2G052671	WRKY domain TF family	

Trait columns (each with bi-parental and MAGIC sub-columns): LL, Lwe, LA, Lwi, LER, emergence, Tm, Te, LED, DZ, FW, DW.

involved in histone modification (Veiseth et al., 2011; Kumpf et al., 2014). ASHR3 is required for coordinated DNA replication and cell division, and the *ashr3* mutant has a reduced root apical meristem size and primary root size (Kumpf et al., 2014). Moreover, it was shown that expression levels of *ASHR3* are controlled by the E2Fa/E2Fb-DPa TF complex (Kumpf et al.,

2014); in agreement, expression levels of *E2F/DP* TF (*GRMZM2G462623*) correlated positively with final leaf size traits and DZ size in both RIL populations (Fig. 5). Maintenance of epigenetic signatures by setting up the appropriate epigenetic marks is essential to regulate gene expression and establish euchromatin and heterochromatin. Furthermore, histone modification

pathways are intertwined with DNA methylation, for instance by interaction between chromatin modifiers such as SET domain proteins and DNA methyltransferases (Cedar and Bergman, 2009) and/or methyl-CpG-binding domain proteins (MBDs; Zemach and Grafi, 2007), which read out the DNA methylation pattern. The subset of 56 TFs also includes a DNA methyltransferase, of which the expression levels in the DZ were positively correlated with Lwe, LA, DZ size, and the timing-related traits, and a MBD also positively correlated with the traits (Fig. 5). In agreement, the down-regulation of some Arabidopsis *MBD* genes results in developmental defects comparable to the down-regulation of genes with a role in chromatin remodeling and RNA-mediated silencing (Berg et al., 2003; Peng et al., 2006). Also, two *ARGONAUTE* (*AGO*) genes with homology to Arabidopsis *AGO4* involved in RNA-directed DNA methylation (Zilberman et al., 2004) showed a positive correlation with leaf size traits and timing-related traits (Fig. 5). In addition to the covalent histone modifications, chromatin remodeling also depends on ATP-dependent chromatin remodeling complexes that move, eject, or restructure nucleosomes. For instance, the transcription of *GRFs* is regulated by recruitment of the SWITCH/SUCROSE NONFERMENTING (SWI/SNF) chromatin-remodeling complexes to their promoters by the transcriptional coactivator AN3 (Vercruyssen et al., 2014; Nelissen et al., 2015). The phenotypes upon differential expression of *AN3*, *BRAHMA*, or *SWI/SNF-ASSOCIATED PROTEIN73B*, subunits of the SWI/SNF complex, reflect the importance of this chromatin-remodeling complex in the regulation of leaf growth (Farrona et al., 2004; Horiguchi et al., 2005; Vercruyssen et al., 2014), and constitutive overexpression of *GRF1* and *GRF2* also increased leaf and cotyledon size (Kim et al., 2003). In agreement, the subset of 56 TFs enclosed two GRFs that displayed a positive correlation with leaf size- and timing-related traits (Fig. 5).

More than one-third of the 56 TFs that were correlated with leaf-related traits in the two populations had homologs with a known role in growth, while most of the other TFs had an unknown function. We primarily identified genes required for hormone signaling, leaf architecture, and chromatin remodeling, next to TFs involved in other processes, such as Suc signaling (homeobox TF family; Hanson et al., 2001) and cell cycle regulation (Trihelix TF; Breuer et al., 2012).

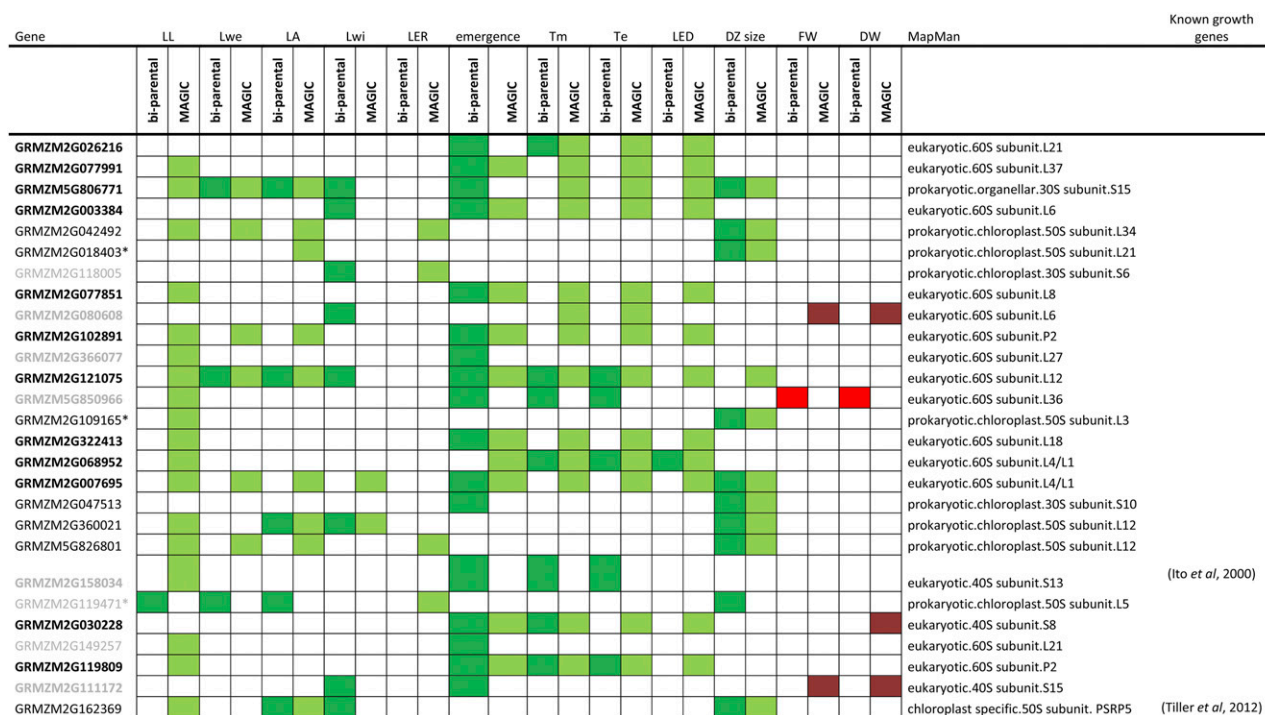### Protein Synthesis Is Negatively Correlated to Leaf Growth

In the functional category protein synthesis, all 26 genes shared between the two populations are ribosomal proteins. Ribosomes provide the basis for protein production, which is essential to sustain cell growth. Therefore, the majority of the genes that encode for ribosomal proteins are highly expressed at the base of the leaf in the DZ (Li et al., 2010), and all selected ribosomal

proteins in our data set, except for the chloroplast ribosomal proteins that showed the highest expression toward the elongation zone, were specifically expressed in the DZ, as determined by the Bio-Analytic Resource expression viewer (Fig. 6). The energy status of the cell tunes the transcription of ribosomal RNA and the production and maintenance of ribosomal proteins, which are substantial indirect costs of protein synthesis. Since protein synthesis is one of the most energy-consuming processes in the cell, one can expect selective pressure to achieve a frugal use of the translational machinery (Perry, 2007). Thus, a more efficient translational machinery that minimizes the indirect costs of protein synthesis is likely to allow a higher rate of cell proliferation and growth (Lempiäinen and Shore, 2009; Piques et al., 2009), a possible explanation for the anticorrelation we observe between transcript levels of genes encoding for ribosomal proteins and leaf size and timing traits.

The importance of the translational machinery is reflected in the effect that many mutations in ribosomal proteins have on leaf development (for review, see Byrne, 2009; Horiguchi et al., 2012). For instance, Arabidopsis *RPS13A* encodes a 40S ribosomal protein S13 involved in early leaf development. An insertion mutant of *RPS13A* gives rise to a whole range of phenotypic abnormalities, including an altered leaf shape of the first leaves and an increased number of leaves compared with the wild type (Ito et al., 2000). In our data set, transcript levels of the homologous maize gene *GRMZM2G158034* were anticorrelating with the leaf size and timing traits in both populations (Fig. 6). Also, the expression levels of several chloroplast ribosomal proteins were anticorrelated with the leaf size traits (Fig. 6). Many of the nucleus-encoded components of the plastid ribosomes are essential for plant growth and development, since their absence results in diverse phenotypic effects, such as embryo lethality, paleness, and reduced overall sizes (Magnard et al., 2004; Asakura et al., 2012; Romani et al., 2012). The Arabidopsis TF *CHLOROPLAST IMPORT APPARATUS2* (*CIA2*) was shown to up-regulate the expression of genes encoding chloroplast ribosomal proteins to accomplish the high protein demands of chloroplasts (Sun et al., 2009). Three of the eight chloroplast ribosomal proteins in our data set were homologs of the Arabidopsis genes up-regulated by CIA2. Also, the maize homolog of *CIA2*, *GRMZM2G062885*, was negatively correlated with leaf size traits (Fig. 4).

Leaf Growth Is Strongly Correlated with Cell Wall Characteristics

To allow cells to grow, cell wall expansion is indispensable, and this was also reflected in the overrepresentation of the functional category cell wall synthesis and degradation for genes with expression levels correlated with leaf size traits. The BioArray tool revealed that the 15 correlating genes in this functional category

Gene	MapMan	Known growth genes
GRMZM2G026216	eukaryotic.60S subunit.L21	
GRMZM2G077991	eukaryotic.60S subunit.L37	
GRMZM5G806771	prokaryotic.organellar.30S subunit.S15	
GRMZM2G003384	eukaryotic.60S subunit.L6	
GRMZM2G042492	prokaryotic.chloroplast.50S subunit.L34	
GRMZM2G018403*	prokaryotic.chloroplast.50S subunit.L21	
GRMZM2G118005	prokaryotic.chloroplast.30S subunit.S6	
GRMZM2G077851	eukaryotic.60S subunit.L8	
GRMZM2G080608	eukaryotic.60S subunit.L6	
GRMZM2G102891	eukaryotic.60S subunit.P2	
GRMZM2G366077	eukaryotic.60S subunit.L27	
GRMZM2G121075	eukaryotic.60S subunit.L12	
GRMZM5G850966	eukaryotic.60S subunit.L36	
GRMZM2G109165*	prokaryotic.chloroplast.50S subunit.L3	
GRMZM2G322413	eukaryotic.60S subunit.L18	
GRMZM2G068952	eukaryotic.60S subunit.L4/L1	
GRMZM2G007695	eukaryotic.60S subunit.L4/L1	
GRMZM2G047513	prokaryotic.chloroplast.30S subunit.S10	
GRMZM2G360021	prokaryotic.chloroplast.50S subunit.L12	
GRMZM5G826801	prokaryotic.chloroplast.50S subunit.L12	
GRMZM2G158034	eukaryotic.40S subunit.S13	(Ito et al, 2000)
GRMZM2G119471*	prokaryotic.chloroplast.50S subunit.L5	
GRMZM2G030228	eukaryotic.40S subunit.S8	
GRMZM2G149257	eukaryotic.60S subunit.L21	
GRMZM2G119809	eukaryotic.60S subunit.P2	
GRMZM2G111172	eukaryotic.40S subunit.S15	
GRMZM2G162369	chloroplast specific.50S subunit. PSRP5	(Tiller et al, 2012)

Trait columns (each with bi-parental and MAGIC subcolumns): LL, Lwe, LA, Lwi, LER, emergence, Tm, Te, LED, DZ size, FW, DW.

Figure 6. Ribosomal proteins with expression profiles correlating or anticorrelating with at least one of the traits in both populations. Bright red indicates positive correlation in the biparental population, dark red indicates positive correlation in the MAGIC population, dark green indicates negative correlation in the biparental population, and light green indicates negative correlation in the MAGIC population. Asterisks indicate genes that are homologs of the Arabidopsis chloroplast ribosomal genes up-regulated by *CIA2* (Sun et al., 2009). DZ-specific genes are indicated in boldface (Li et al., 2010). DW, Dry weight; FW, fresh weight.

are all highly expressed in the DZ (Li et al., 2010). Five of these genes are involved in cellulose synthesis, of which three were positively correlated with the traits while two showed anticorrelation (Fig. 7). Expression levels of the catalytic subunits of the cellulose synthase complex *CELLULOSE SYNTHASE3* (*ZmCESA3*; *GRMZM2G039454*), *ZmCESA5* (*GRMZM2G111642*), and *GRMZM2G099101* were positively correlating with leaf size traits (Fig. 7). Mutations in the respective Arabidopsis orthologs *CESA1*, *CESA3*, and *KORRIGAN* (*KOR*), which interact with specific CESA complexes (Mansoori et al., 2014), cause an abnormal plant morphology and severe dwarfism due to defects in cell wall formation (Sato et al., 2001; Beeckman et al., 2002; Persson et al., 2007). On the other hand, expression levels of *GRMZM2G027794* and *GRMZM2G074792*, which show homology to the CESA-like C family in Arabidopsis, were negatively correlated with leaf size traits (Fig. 7). This family is most likely involved in the biosynthesis of the glucan backbone of the hemicellulosic polysaccharide xyloglucan rather than cellulose (Liepman and Cavalier, 2012). Lower amounts of xyloglucans in growing tissue possibly increase the accessibility of the primary cell wall for cell wall-loosening enzymes to promote cell wall extension and cell expansion (Pauly et al., 2001). In addition, four genes, *GRMZM2G165357*, *GRMZM2G007404*,

GRMZM2G328500, and *GRMZM5G862540*, involved in the biosynthesis of UDP-Xyl (Harper and Bar-Peled, 2002; Kärkönen et al., 2005; Reboul et al., 2011), a nucleotide sugar required for the synthesis of diverse plant cell wall polysaccharides including xyloglucan, had expression levels in the DZ that also negatively correlated with the leaf size traits (Fig. 7).

In addition to cell wall biosynthesis genes, genes involved in cell wall degradation were also identified. Expression levels of the cell wall-loosening enzyme endo-1,4-β-glucanase/cellulase (*GRMZM2G331566*) were positively correlated with LL and timing-related traits in our data set (Fig. 7). In accordance, it was demonstrated in transgenic Arabidopsis plants that the expression of poplar (*Populus* spp.) *CELLULASE1* resulted in enhanced growth rates (Park et al., 2003). Expression levels of *β-EXPANSIN4*, another cell wall-loosening enzyme, were negatively correlated with leaf size traits (Fig. 7), although up- and down-regulation of expansin expression in Arabidopsis and rice resulted in larger and smaller leaves, respectively (Cho and Cosgrove, 2000; Choi et al., 2003; Goh et al., 2012). However, more pleiotropic phenotypes were observed after constitutive modification of expansin gene expression, including a reduction in overall plant growth (Rochange and McQueen-Mason, 2000), demonstrating that the effect of expansin expression on leaf growth is
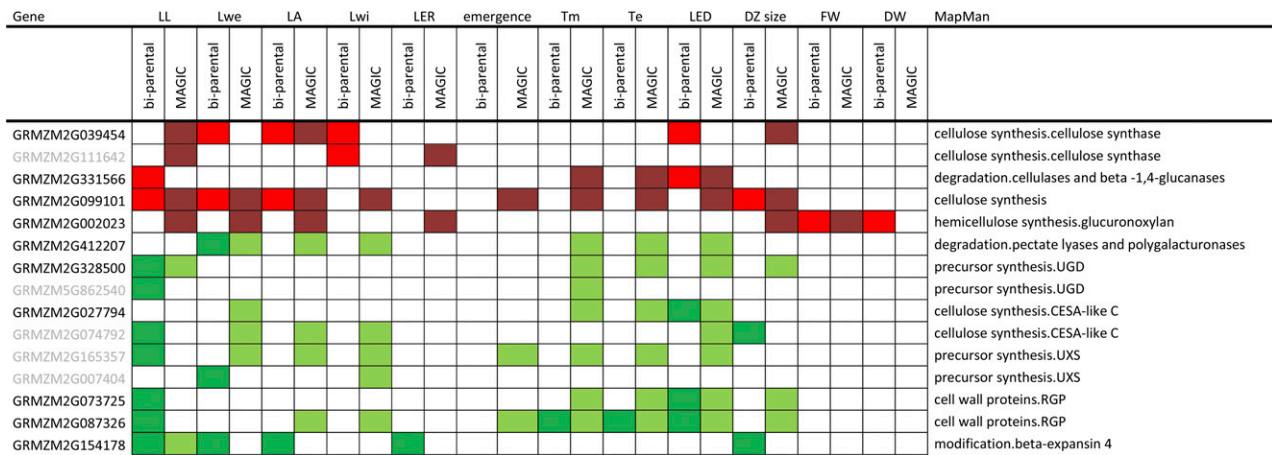
Figure 7. Cell wall-related proteins with expression profiles correlating or anticorrelating with at least one of the traits in both populations. Bright red indicates positive correlation in the biparental population, dark red indicates positive correlation in the MAGIC population, dark green indicates negative correlation in the biparental population, and light green indicates negative correlation in the MAGIC population. DW, Dry weight; FW, fresh weight.

Gene	MapMan
GRMZM2G039454	cellulose synthesis.cellulose synthase
GRMZM2G111642	cellulose synthesis.cellulose synthase
GRMZM2G331566	degradation.cellulases and beta -1,4-glucanases
GRMZM2G099101	cellulose synthesis
GRMZM2G002023	hemicellulose synthesis.glucuronoxylan
GRMZM2G412207	degradation.pectate lyases and polygalacturonases
GRMZM2G328500	precursor synthesis.UGD
GRMZM5G862540	precursor synthesis.UGD
GRMZM2G027794	cellulose synthesis.CESA-like C
GRMZM2G074792	cellulose synthesis.CESA-like C
GRMZM2G165357	precursor synthesis.UXS
GRMZM2G007404	precursor synthesis.UXS
GRMZM2G073725	cell wall proteins.RGP
GRMZM2G087326	cell wall proteins.RGP
GRMZM2G154178	modification.beta-expansin 4

Trait columns (each split into bi-parental and MAGIC): LL, Lwe, LA, Lwi, LER, emergence, Tm, Te, LED, DZ size, FW, DW.

context dependent and influenced by the growth phase of the leaf (Sloan et al., 2009).

Intriguingly, for many of the cell wall-related genes that were negatively correlated with leaf and shoot size traits in our data set, down-regulation of these genes or their orthologs has been shown previously to result in a growth reduction (Sato et al., 2001; Roberts et al., 2004; Rautengarten et al., 2011) or even embryo lethality (Goubet et al., 2003). We hypothesize that the difference between the direction of the correlation in our data set and the phenotypes of Arabidopsis homologs might be due to the comparison of more subtle variations in expression because of allelic effects in natural variants with more drastic effects of knockout or constitutive overexpression often in one genetic background in Arabidopsis. Most likely, to obtain growth-promoting effects, more subtle changes in expression levels should be applied during specific phases of development and/or by combinatorial perturbation of several genes.

Toward a Robust Growth Regulatory Network

Of the 226 genes we identified with expression levels in the DZ (anti)correlating with at least one of the traits in both populations, some were described previously to be associated with leaf size and growth. However, the majority of these genes was not identified until now as linked to growth, and 48 of these genes even had no assigned function. To obtain a better insight into the putative coregulation of these 226 genes, we used CORNET Corn (De Bodt et al., 2012) to identify networks of coexpressed genes based on the expression of these query genes in two publicly available expression compendia. Additionally, protein-protein interactions based on experimental and computational data (primarily inferred from Arabidopsis) were added to this network.

The resulting network incorporates 185 genes and 943 edges (Fig. 8). Of the other 41 genes, for seven no reliable probe sets were identified on the arrays used to generate the CORNET data sets, while for 34 genes no coexpression or interaction links were found.

Functional information and correlation to the three trait groups were visualized in the network for each gene, and four subnetworks were determined using CytoCluster (Fig. 8). Two of these subnetworks were enriched in the functional category protein synthesis. ribosomal proteins; subnetwork 1 contained genes anticorrelating primarily with the timing traits, and subnetwork 4 was primarily anticorrelated with leaf size traits (Fig. 8). The genes within the two subnetworks were highly connected to each other and to a limited set of other genes. For subnetwork 1, one of these other genes, *GRMZM2G038032*, shows homology to Arabidopsis *RECEPTOR FOR ACTIVATED C PROTEIN KINASE1* (*RACK1*) genes involved in ribosome biogenesis (Guo et al., 2011); it was shown that loss-of-function mutations in *RACK1* genes in Arabidopsis severely affect rosette leaf production and root growth (Guo and Chen, 2008). The ribosomal genes in this first subnetwork were also highly connected to *GRMZM2G067877*, a homolog of an Arabidopsis mitochondrial adenine nucleotide transporter (*ADNT1*) that plays a role in energy supply in heterotrophic tissues. This protein catalyzes the exchange between cytosolic AMP and intramitochondrial ATP, and plants with decreased *ADNT1* expression show an inhibition of root growth (Palmieri et al., 2008). A third gene that was coexpressed with the ribosomal genes in subnetwork 1 is *GRMZM2G389768*, a putative *COLD SHOCK DOMAIN* (*CSP*) gene. In Arabidopsis it was shown that *CSP1* associates with polysomes by binding to a specific set of mRNAs and acts as a chaperone under low temperatures. *CSP1* primarily binds mRNAs encoding for energy-consuming processes, such as ribosome
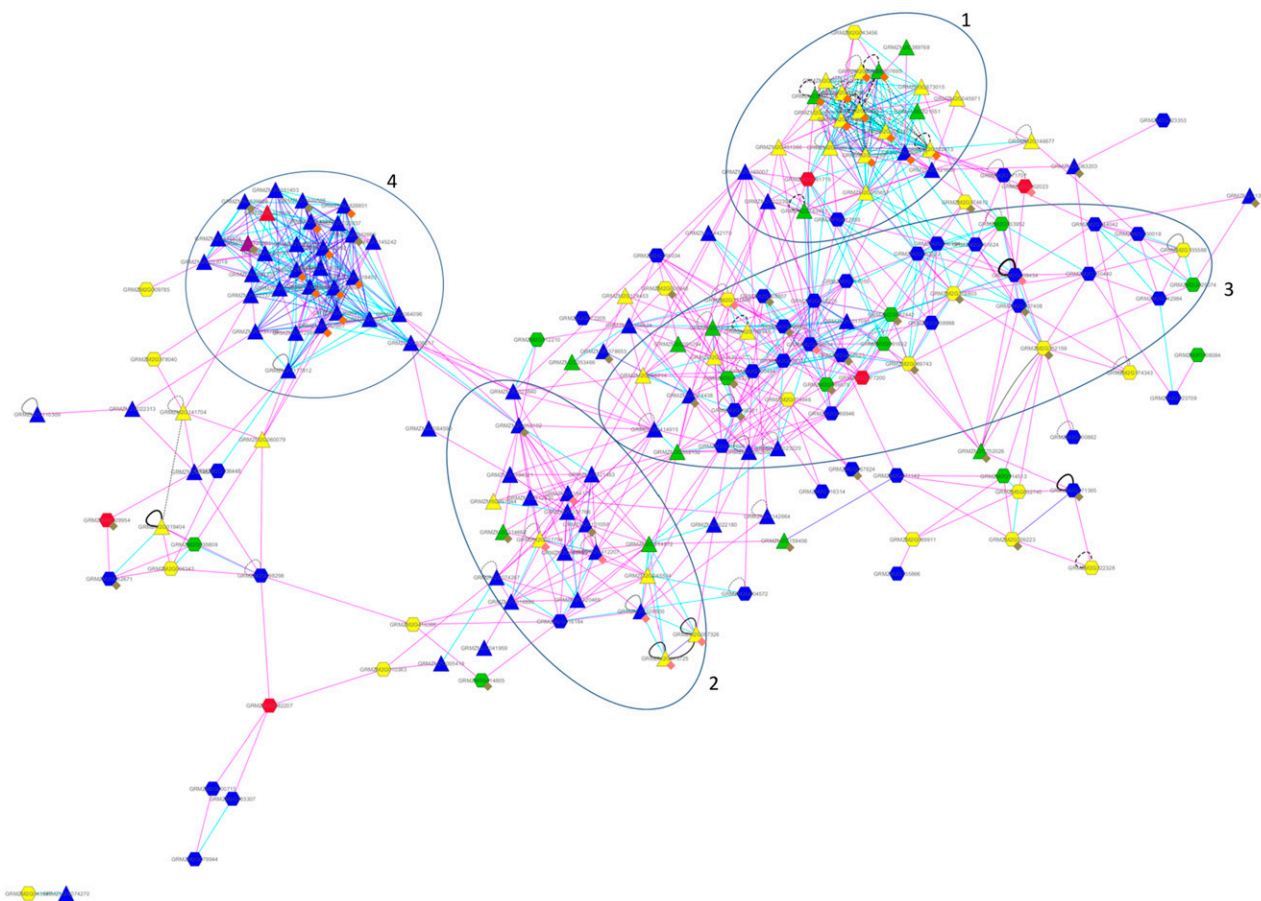
Figure 8. Coexpression and interaction network of genes with expression levels in the DZ correlating with leaf size traits in both populations. Negatively correlating genes are represented by triangles and positively correlating genes by hexagons. Node colors represent correlation with timing traits (yellow), leaf size traits (blue), shoot traits (red), timing and leaf size traits (green), and leaf size and shoot traits (purple). Small diamonds attached to the nodes represent the functional classification of the genes; orange squares indicate genes encoding ribosomal proteins, brown squares are TFs, and pink squares are cell wall-related genes; other functional categories are not indicated. Edges colored blue connect coexpressed genes with a PCC of at least 0.8, pink edges represent a PCC between 0.7 and 0.8, while black edges represent protein-protein interactions that were experimentally validated (solid lines) or computationally predicted (dashed lines). Subnetworks as determined by CytoCluster are indicated by numbers.

biogenesis, to maintain the translation of these specific mRNAs under stress conditions (Juntawong et al., 2013). Thus, this first subnetwork of coexpressed genes seems to be linked to energy consumption and supply, suggesting that the duration of leaf growth is associated with energy availability, as the genes in this subnetwork are anticorrelated with timing traits.

The network contained a second subset of strongly coexpressed genes encoding ribosomal proteins and a limited number of other negatively correlated genes, subnetwork 4 (Fig. 8). In contrast to subnetwork 1, these genes showed anticorrelating primarily to the leaf size traits (Fig. 8). Of the 31 nodes in this subnetwork, nine were ribosomal proteins all targeted to the chloroplasts. For most of these genes, the effect of perturbed expression was not analyzed before now (Tiller and Bock, 2014). However, two of the Arabidopsis orthologs of these ribosomal proteins, RPL21C and RPL3, were shown to be essential for plastid development and

embryogenesis (Yin et al., 2012; Tiller and Bock, 2014), while reduced gene expression of the plastid-specific ribosomal protein PSRP5 resulted in severely delayed plant growth due to reduced plastid translation (Tiller et al., 2012). Additionally, this subnetwork contained one GATA TF (*GRMZM2G039586*) homologous to Arabidopsis *GCN*, described to function in chloroplast development, likely by regulating chloroplast division (Chiang et al., 2012). Interestingly, the majority of the other genes in this subnetwork were chloroplast targeted and involved in chloroplast development and/or functioning. We identified genes functioning in chloroplast biogenesis, for instance tetrapyrrole biosynthesis genes (Huang et al., 2009; Quesada et al., 2013) and the FZO-like protein FZL coding for a dynamin-related membrane-remodeling protein (Gao et al., 2006); genes with metabolic functions in chloroplast coding, for instance, for components of the NAD(P)H dehydrogenase complex (Ishida et al., 2009) essential for the supply

of ATP for photosynthesis (Endo et al., 2008); and genes involved in plastid gene expression, such as the ribosomal proteins, components of the plastid-encoded RNA polymerase complex, the pfkB-type carbohydrate kinase FRUCTOKINASE-LIKE PROTEIN (Gilkerson et al., 2012), *MurE* (Garcia et al., 2008), and *PLASTID TRANSCRIPTIONALLY ACTIVE CHROMOSOME6* (Pfalz et al., 2006), CIA2 (Sun et al., 2009), genes involved in chloroplast protein import (Chiu and Li, 2008), and pentatricopeptide repeat proteins (Liu et al., 2013a). As a consequence, many mutants in these genes are chlorotic, white, or pale green due to abnormal plastid development and reduced photosynthetic competence. However, evidence for the impact of chloroplast development and plastid protein synthesis on leaf development and morphology independent of photosynthetic capacity has been suggested for a long time (for review, see Tiller and Bock, 2014).

Since the genes with a role in leaf development that are currently described are nucleus encoded, it seems likely that this effect of plastid translation on leaf development is the consequence of plastid-nucleus communication known as chloroplast retrograde signaling (Larkin, 2014). Recently, it was shown that chloroplast retrograde signaling regulates the spatial expression levels of genes involved in the expansion of leaf primordia, probably to avoid the expansion of leaves with reduced photosynthesis due to impaired plastid activity (Tameshige et al., 2013). Furthermore, in Arabidopsis, it was postulated that chloroplast retrograde signaling is an important regulator of the onset of cell expansion and photosynthesis (Andriankaja et al., 2012). Although the chloroplasts are still undifferentiated in the most basal part of the DZ we sampled for RNA sequencing (Majeran et al., 2010), it can be assumed that signaling between plastids and the nucleus starts early on, as plastid biogenesis is highly coordinated with organ development to ensure the presence of the appropriate number of plastids of the correct type in each stage of development (Terry and Smith, 2013). Subnetwork 4 with nucleus-encoded genes targeted to the chloroplasts and functioning in chloroplast development, and some possibly also in chloroplast retrograde signaling (Strand et al., 2003; Garcia et al., 2008; Gilkerson et al., 2012), showed a variation in expression levels in both RIL populations. This expression variation in the DZ between RILs and the anticorrelation with leaf size traits suggests an early coordination of extrachloroplastic processes with chloroplast function via chloroplast retrograde signaling.

Besides the two highly intraconnected subnetworks of genes encoding ribosomal proteins, two other subnetworks were identified. Subnetwork 2 consisted of 22 nodes, primarily anticorrelated with leaf size traits (Fig. 8). This subnetwork was enriched in cell wall biogenesis and degradation: six of the 22 genes in this subnetwork were involved in this process, and all negatively correlated with leaf size or timing traits. These cell wall-related genes as well as other genes of subnetwork 2 were coexpressed with *GRMZM2G045534*, an

ATP-citrate lyase whose down-regulation of Arabidopsis orthologs results in pleiotropic phenotypes, including reduced size (Fatland et al., 2005). Also, three TFs were highly coexpressed with the genes in subnetwork 2: *GATA* TF (*GRMZM2G101058*) described above, a *bZIP* TF (*GRMZM2G052102*) of which the Arabidopsis orthologous mutant shows cell wall defects in pollen (Gibalová et al., 2009), and a *TRIHELIX* TF (*GRMZM2G314660*). The latter shows homology to Arabidopsis *GTL1*, a master regulator that negatively regulates cell growth (Breuer et al., 2012). Other examples of genes in this subnetwork that were already functionally annotated were *ZmPIN1b*, an auxin efflux carrier (Carraro et al., 2006), and *Zmβ-GLUCOSIDASE1*, involved in the (in)activation of cytokinins (Brzobohatý et al., 1993).

Subnetwork 3 consisted of 45 genes that were primarily positively correlated to leaf size and timing traits (Fig. 8). This subnetwork was enriched for two functional categories, regulation of transcription (12 genes) and cell wall synthesis and degradation (three genes). The node with the most edges in this subnetwork was a cell wall-related gene, *KOR* (*GRMZM2G099101*), and was coexpressed with eight TFs: three *bHLH* TFs, GRMZM2G074438, GRMZM2G128807, and GRMZM2G158281, the latter showing orthology to Arabidopsis *LONESOME HIGHWAY*, which is required for establishing and maintaining the normal vascular cell number and pattern in roots (Ohashi-Ito and Bergmann, 2007); two SET domain TFs, *GRMZM2G409224* and *GRMZM2G318803*, the latter being a homolog of Arabidopsis *SUVR4*; *E2F/DP* (*GRMZM2G462623*) and *GRF* (*GRMZM2G099862*), both having homologs in Arabidopsis with known roles in leaf development (De Veylder et al., 2002; Kim et al., 2003); and an *AGO* gene with homology to Arabidopsis *AGO4* (*GRMZM2G589579*). Other genes coexpressed in this subnetwork with known annotations include the cell cycle gene *CYCLIN A2* (*GRMZM2G017081*), involved in vein development in Arabidopsis (Donner and Scarpella, 2013), and *BRASSINOSTEROID SIGNALING KINASE2* (*GRMZM2G054634*), affecting growth through its role in the initial steps of brassinosteroid signal transduction in Arabidopsis (Sreeramulu et al., 2013). Still other genes in this subnetwork were primarily linked to metabolic processes and/or are not well described to date.

Within the set of 226 genes identified in the two-way and eight-way RIL populations, we found 185 genes to be coexpressed and four subnetworks could be distinguished, of which two were enriched in the functional category protein synthesis.ribosomal proteins. Of the 185 genes, 32 were TFs, and for some a function in leaf development and growth had already been described (see above). Coexpression relationships between these TFs and other genes may suggest potential regulatory influences; however, clear causal links between these TFs and potential targets cannot be established from the coexpression network alone, and further analyses are necessary to confirm these links.

CONCLUSION

In this study, we report an integrated analysis of transcript measurements in proliferative tissue and in-depth phenotyping of leaf size parameters of 197 RILs belonging to two different maize segregating populations to establish how variation in transcript levels relates to phenotypic changes. A set of 226 genes was identified for which the expression levels in the DZ correlated significantly with final leaf size and timing or shoot traits in both populations, a strong reduction compared with the 1,740 and 1,364 (anti)correlating genes identified separately in the biparental and MAGIC populations, respectively. Thus, combining data from different populations led to the identification of a limited set of genes, including 56 TFs, that may play a more general role in the molecular networks underlying the establishment of the various phenotypic traits across maize accessions. Of these 226 correlated genes, 185 were present in a highly connected network of coexpressed genes constructed from public expression compendia. The occurrence of several genes known to affect leaf size in this correlated gene list confirms that, already in the dividing cells of growing leaves, the molecular networks that will establish final leaf phenotypes are present. Besides these known genes, genes without a clear function or with no known role in leaf growth were also identified. In summary, our comparative analysis of transcriptome and phenotype variation in two RIL populations supports the conclusions reported earlier for one of the populations (Baute et al., 2015), extends our understanding of system-level processes that are active in leaf growth across different populations, and resulted in the identification of a set of interesting candidate genes for future follow-up studies.

MATERIALS AND METHODS

Plant Growth and Sampling

In this study, a subset of lines of two maize (*Zea mays*) RIL populations was used. A subset of 103 lines of a biparental RIL population derived from a cross between parental lines B73 and H99 (Marino et al., 2009) and a subset of 94 lines of a MAGIC maize population (Dell'Acqua et al., 2015) was phenotyped and sampled for RNA sequencing. The subset of 94 lines was chosen randomly from the set of 529 lines that was genotyped and phenotyped in the field (Dell'Acqua et al., 2015). Phenotyping and RNA sequencing analysis of the biparental RIL population was described by Baute et al. (2015), and analysis of the MAGIC population was performed accordingly. Briefly, plants were grown in a series of experiments in a single growth chamber in a randomized design each time along with B73 (MAGIC population) or B73 and H99 (biparental RIL population) under controlled growth chamber conditions (24°C, 55% relative humidity, light intensity of 170 mmol m^{-2} s^{-1} photosynthetic active radiation, in a 16-h/8-h day/night cycle). Traits measured were final LA, final Lwi, final Lwe, final leaf 4 blade weight, final LL, LER, DZ size of leaf 4, time point of leaf 4 emergence, T_m, T_e, and LED$_{5-e}$. Twenty-seven days after sowing, fresh weight, dry weight, V-stage, and total LN of the whole seedling were determined. In the biparental RIL population, V-stage (a method to determine leaf stage in maize by counting the number of leaves on a plant with visible leaf collars) and total LN were not determined for all 103 RILs but for a selection of 42. Since the results for final Lwe and leaf 4 blade weight were very similar, only results for final Lwe are shown. LER, DZ size, T_m, T_e, and LED$_{5-e}$ were determined as described previously (Rymen et al., 2007; Voorend et al., 2014). Briefly, LER was determined by measuring the leaf length, using the soil level as a reference

point, on a daily basis from the time of emergence of leaf 4 until the leaf was fully grown and calculating the average growth rate during the steady-state growth phase. DZ size was estimated as the distance between the base of the leaf and the most distal mitotic cell in the epidermis that could be visualized after staining with 4',6-diamidino-2-phenylindole. T_m, T_e, and LED$_{5-e}$ were determined using the tool LEAF-E, which allows one to perform nonlinear regression modeling (Voorend et al., 2014). All traits were determined for six to eight plants per RIL, except for DZ size (three plants per RIL) and time point of leaf 4 emergence (19 plants per RIL). Plants were sampled for RNA sequencing simultaneously with the phenotyping. As the size of the DZ differed considerably between the RILs (Supplemental Table S1; between 0.782 and 1.68 cm in the two-way RIL population and between 0.653 and 1.423 cm in the eight-way RIL population) and we wanted to restrict our analysis to fully proliferative leaf tissue, we chose to sample the first 0.5 cm of the most basal part of the leaf during steady-state growth (i.e. 3 d after leaf 4 appearance, always at the same time of the day to minimize diurnal effects). One biological replicate, consisting of proliferative tissue of four plants, was sampled for RNA sequencing. Total RNA was extracted using Trizol (Invitrogen) and subjected to DNA digestion with the RNase-free DNase I kit (Qiagen).

Transcriptome Analysis

RNA sequencing analysis was performed as described before, resulting in a set of 15,051 retained transcripts (Baute et al., 2015). In brief, after library preparation with the TruSeq RNA Sample Preparation Kit version 2 (Illumina), the quality of the raw data was verified with FastQC version 0.9.1 (http://www.bioinformatics.babraham.ac.uk/projects/fastqc/). Next, quality filtering was performed using FASTX-Toolkit version 0.0.13 (http://hannonlab.cshl.edu/fastx_toolkit/). Reads were subsequently mapped to the maize B73 reference genome (5b) using GSNAP (Wu and Nacu, 2010), allowing maximally five mismatches. The concordantly paired reads that uniquely map to the genome were used for quantification on the gene level with htseq-count from the HTSeq.py python package (Anders et al., 2015). To avoid artifacts in the mapping and consequently in transcript quantification because of diversity in the maize inbred lines (Morgante et al., 2007), we selected genes conserved in the eight parental lines of the MAGIC population (Dell'Acqua et al., 2015). Therefore, RNA sequencing data of proliferative tissue for these eight inbred lines were mapped to the B73 reference genome. A coverage cutoff was applied, using the R/Bioconductor package with default HTSFilter parameter settings (Rau et al., 2013), retaining 19,948 genes that were expressed in at least one of the parents. Next, single-nucleotide polymorphism calling was performed, and we selected genes with no more than 1.75% single-nucleotide polymorphisms, resulting in a set of 15,051 genes.

RNA sequencing count data were subsequently normalized for library size with the default normalization method in the DESeq2 package version 1.2.10 (Love et al., 2014). Next, transcripts expressed (nonzero count) in less than 5% of samples were removed. On the remaining transcripts, the inverse hyperbolic sine transformation was applied with the asinh function in R software. Additionally, another filter was applied that removed the 5% least varying transcripts, based on the coefficient of variation, resulting in the selection of 14,255 transcripts in the biparental population and 14,297 transcripts in the MAGIC population.

Correlation Analysis

PCCs among the traits were calculated on the means of the lines in SPSS (SPSS), separately for the two populations.

For correlation analysis between transcript levels and trait variation, PCCs were calculated between each transcript and all traits over all RILs for the two populations separately. As described before (Baute et al., 2015), for each trait in each population, the $q_{0.01}$ and $q_{0.99}$ quantiles of the set of transcript-trait PCC values were calculated and compared with a reference correlation coefficient. These reference correlation coefficients were determined by permuting the trait values 1,000 times and calculating the $q_{0.01}$ and $q_{0.99}$ quantiles for each permutation. The mean $q_{0.01}$ and $q_{0.99}$ quantiles after permutation, $q_{0.01,random}$ and $q_{0.99,random}$, were taken as the reference correlation coefficients expected by chance across all RIL samples of one population. The permutation of each trait was conducted in R software using the corr function for the calculation of PCC and the sample function for trait permutation. We focused on the genes with correlation coefficients lower and higher than the (real) $q_{0.01}$ and $q_{0.99}$ quantiles of the set of transcript-trait correlation coefficient values, respectively, referred to as the anticorrelating and correlating gene sets, respectively.

Principal component analysis was performed as a dimensionality reduction technique on the centered and scaled phenotype data, using the prcomp function in R.

To determine whether the number of (anti)correlating genes in the intersection of both populations was higher than expected by chance, we used hypergeometric tests.

Visualization of Expression Patterns

The expression patterns of the set of 226 genes (anti)correlating with at least one trait in both populations and the phenotypic measurements for all RILs were visualized in MeV (Saeed et al., 2003). Data were adjusted by normalizing the genes/row, and color scale limits were set at −3 and +3 as lower limit and upper limit, respectively, since these numbers approached the minimal and maximal data values after normalization. Next, we performed hierarchical clustering of the RILs, based on Euclidean distance and average linkage clustering, to visualize the gradient in expression levels and phenotypic measurements over all RILs.

Functional Enrichment Analysis

Functional enrichment analyses were based on pathways defined in MapMan (Thimm et al., 2004) and performed as described before (Baute et al., 2015).

Network Analysis

Coexpression analysis between the 226 genes for which expression levels in the DZ (anti)correlated with at least one of the traits in both populations was performed with the online tool CORNET (De Bodt et al., 2012), but with its in-house version, where the probe sets of publicly available Affymetrix and Nimblegen expression data sets for maize are mapped to gene models B73_RefGen_v2. For our analysis, we selected both expression data sets, Affymetrix and Nimblegen. The generated coexpression network was based on PCCs of 0.7 and higher, and protein-protein interactions between query genes based on both experimental and predicted data from CORNET were included and visualized in Cytoscape (Shannon et al., 2003). Subnetworks were identified using HC-PIN (Wang et al., 2011) in CytoCluster with standard settings and a ComplexSize threshold of 10.

Phenotypic measurements are included in Supplemental Table S4.

Sequence data from this article can be found in the GenBank/EMBL data libraries under accession numbers E-MTAB-3965.

Supplemental Data

The following supplemental materials are available.

Supplemental Figure S1. PCA analysis of the phenotype data.

Supplemental Figure S2. Histograms of the leaf size and seedling related traits in the bi-parental RIL and MAGIC RIL population.

Supplemental Figure S3. Enrichment of functional categories for correlating and anti-correlating genes in the bi-parental and MAGIC RIL populations.

Supplemental Table S1. Mean, maximum, minimum and percentage difference of the traits within the two populations.

Supplemental Table S2. Pearson CC for the analyzed traits, grouped as leaf size, shoot related and timing related traits combined for bi-parental and MAGIC RIL populations.

Supplemental Table S3. Genes with expression levels (anti-)correlating with at least one of the traits in one of the populations.

Supplemental Table S4. Phenotypic measurements for the MAGIC population.

LITERATURE CITED

Aguilar-Martínez JA, Sinha N (2013) Analysis of the role of Arabidopsis class I TCP genes AtTCP7, AtTCP8, AtTCP22, and AtTCP23 in leaf development. Front Plant Sci **4:** 406

Anders S, Pyl PT, Huber W (2015) HTSeq - a Python framework to work with high-throughput sequencing data. Bioinformatics **31:** 166–169

Andorf S, Meyer RC, Selbig J, Altmann T, Repsilber D (2012) Integration of a systems biological network analysis and QTL results for biomass heterosis in Arabidopsis thaliana. PLoS ONE **7:** e49951

Andriankaja M, Dhondt S, De Bodt S, Vanhaeren H, Coppens F, De Milde L, Mühlenbock P, Skirycz A, Gonzalez N, Beemster GT, et al (2012) Exit from proliferation during leaf development in Arabidopsis thaliana: a not-so-gradual process. Dev Cell **22:** 64–78

Asakura Y, Galarneau E, Watkins KP, Barkan A, van Wijk KJ (2012) Chloroplast RH3 DEAD box RNA helicases in maize and Arabidopsis function in splicing of specific group II introns and affect chloroplast ribosome biogenesis. Plant Physiol **159:** 961–974

Bai MY, Shang JX, Oh E, Fan M, Bai Y, Zentella R, Sun TP, Wang ZY (2012) Brassinosteroid, gibberellin and phytochrome impinge on a common transcription module in Arabidopsis. Nat Cell Biol **14:** 810–817

Baute J, Herman D, Coppens F, De Block J, Slabbinck B, Dell'Acqua M, Pè ME, Maere S, Nelissen H, Inzé D (2015) Correlation analysis of the transcriptome of growing leaves with mature leaf parameters in a maize RIL population. Genome Biol **16:** 168

Beeckman T, Przemeck GK, Stamatiou G, Lau R, Terryn N, De Rycke R, Inzé D, Berleth T (2002) Genetic complexity of cellulose synthase A gene function in Arabidopsis embryogenesis. Plant Physiol **130:** 1883–1893

Berg A, Meza TJ, Mahić M, Thorstensen T, Kristiansen K, Aalen RB (2003) Ten members of the Arabidopsis gene family encoding methyl-CpG-binding domain proteins are transcriptionally active and at least one, AtMBD11, is crucial for normal development. Nucleic Acids Res **31:** 5291–5304

Breuer C, Morohashi K, Kawamura A, Takahashi N, Ishida T, Umeda M, Grotewold E, Sugimoto K (2012) Transcriptional repression of the APC/C activator CCS52A1 promotes active termination of cell growth. EMBO J **31:** 4488–4501

Brzobohatý B, Moore I, Kristoffersen P, Bako L, Campos N, Schell J, Palme K (1993) Release of active cytokinin by a beta-glucosidase localized to the maize root meristem. Science **262:** 1051–1054

Byrne ME (2009) A role for the ribosome in development. Trends Plant Sci **14:** 512–519

Carraro N, Forestan C, Canova S, Traas J, Varotto S (2006) ZmPIN1a and ZmPIN1b encode two novel putative candidates for polar auxin transport and plant architecture determination of maize. Plant Physiol **142:** 254–264

Cavanagh C, Morell M, Mackay I, Powell W (2008) From mutations to MAGIC: resources for gene discovery, validation and delivery in crop plants. Curr Opin Plant Biol **11:** 215–221

Cedar H, Bergman Y (2009) Linking DNA methylation and histone modification: patterns and paradigms. Nat Rev Genet **10:** 295–304

Chiang YH, Zubo YO, Tapken W, Kim HJ, Lavanway AM, Howard L, Pilon M, Kieber JJ, Schaller GE (2012) Functional characterization of the GATA transcription factors GNC and CGA1 reveals their key role in chloroplast development, growth, and division in Arabidopsis. Plant Physiol **160:** 332–348

Chiu CC, Li HM (2008) Tic40 is important for reinsertion of proteins from the chloroplast stroma into the inner membrane. Plant J **56:** 793–801

Cho HT, Cosgrove DJ (2000) Altered expression of expansin modulates leaf growth and pedicel abscission in Arabidopsis thaliana. Proc Natl Acad Sci USA **97:** 9783–9788

Choi D, Lee Y, Cho HT, Kende H (2003) Regulation of expansin gene expression affects growth and development in transgenic rice plants. Plant Cell **15:** 1386–1398

Churchill GA, Airey DC, Allayee H, Angel JM, Attie AD, Beatty J, Beavis WD, Belknap JK, Bennett B, Berrettini W, et al (2004) The Collaborative Cross, a community resource for the genetic analysis of complex traits. Nat Genet **36:** 1133–1137

De Bodt S, Hollunder J, Nelissen H, Meulemeester N, Inzé D (2012) CORNET 2.0: integrating plant coexpression, protein-protein interactions, regulatory interactions, gene associations and functional annotations. New Phytol **195:** 707–720

Dell'Acqua M, Gatti DM, Pea G, Cattonaro F, Coppens F, Magris G, Hlaing AL, Aung HH, Nelissen H, Baute J, et al (2015) Genetic properties of the MAGIC maize population: a new platform for high definition QTL mapping in Zea mays. Genome Biol **16**: 167

De Veylder L, Beeckman T, Beemster GT, de Almeida Engler J, Ormenese S, Maes S, Naudts M, Van Der Schueren E, Jacqmard A, Engler G, et al (2002) Control of proliferation, endoreduplication and differentiation by the Arabidopsis E2Fa-DPa transcription factor. EMBO J **21**: 1360–1368

Dignat G, Welcker C, Sawkins M, Ribaut JM, Tardieu F (2013) The growths of leaves, shoots, roots and reproductive organs partly share their genetic control in maize plants. Plant Cell Environ **36**: 1105–1119

Donner TJ, Scarpella E (2013) Transcriptional control of early vein expression of CYCA2;1 and CYCA2;4 in Arabidopsis leaves. Mech Dev **130**: 14–24

Endo T, Ishida S, Ishikawa N, Sato F (2008) Chloroplastic NAD(P)H dehydrogenase complex and cyclic electron transport around photosystem I. Mol Cells **25**: 158–162

Farrona S, Hurtado L, Bowman JL, Reyes JC (2004) The Arabidopsis thaliana SNF2 homolog AtBRM controls shoot development and flowering. Development **131**: 4965–4975

Fatland BL, Nikolau BJ, Wurtele ES (2005) Reverse genetic characterization of cytosolic acetyl-CoA generation by ATP-citrate lyase in *Arabidopsis*. Plant Cell **17**: 182–203

Gao H, Sage TL, Osteryoung KW (2006) FZL, an FZO-like protein in plants, is a determinant of thylakoid and chloroplast morphology. Proc Natl Acad Sci USA **103**: 6759–6764

Garcia M, Myouga F, Takechi K, Sato H, Nabeshima K, Nagata N, Takio S, Shinozaki K, Takano H (2008) An Arabidopsis homolog of the bacterial peptidoglycan synthesis enzyme MurE has an essential role in chloroplast development. Plant J **53**: 924–934

Gibalová A, Renák D, Matczuk K, Dupl'áková N, Cháb D, Twell D, Honys D (2009) AtbZIP34 is required for Arabidopsis pollen wall patterning and the control of several metabolic pathways in developing pollen. Plant Mol Biol **70**: 581–601

Gilkerson J, Perez-Ruiz JM, Chory J, Callis J (2012) The plastid-localized pfkB-type carbohydrate kinases FRUCTOKINASE-LIKE 1 and 2 are essential for growth and development of Arabidopsis thaliana. BMC Plant Biol **12**: 102

Godfray HC, Beddington JR, Crute IR, Haddad L, Lawrence D, Muir JF, Pretty J, Robinson S, Thomas SM, Toulmin C (2010) Food security: the challenge of feeding 9 billion people. Science **327**: 812–818

Goh HH, Sloan J, Dorca-Fornell C, Fleming A (2012) Inducible repression of multiple expansin genes leads to growth suppression during leaf development. Plant Physiol **159**: 1759–1770

Gonzalez N, De Bodt S, Sulpice R, Jikumaru Y, Chae E, Dhondt S, Van Daele T, De Milde L, Weigel D, Kamiya Y, et al (2010) Increased leaf size: different means to an end. Plant Physiol **153**: 1261–1279

Gonzalez N, Vanhaeren H, Inzé D (2012) Leaf size control: complex coordination of cell division and expansion. Trends Plant Sci **17**: 332–340

Goubet F, Misrahi A, Park SK, Zhang Z, Twell D, Dupree P (2003) AtCSLA7, a cellulose synthase-like putative glycosyltransferase, is important for pollen tube growth and embryogenesis in Arabidopsis. Plant Physiol **131**: 547–557

Guo J, Chen JG (2008) RACK1 genes regulate plant development with unequal genetic redundancy in Arabidopsis. BMC Plant Biol **8**: 108

Guo J, Wang S, Valerius O, Hall H, Zeng Q, Li JF, Weston DJ, Ellis BE, Chen JG (2011) Involvement of Arabidopsis RACK1 in protein translation and its regulation by abscisic acid. Plant Physiol **155**: 370–383

Hanson J, Johannesson H, Engström P (2001) Sugar-dependent alterations in cotyledon and leaf development in transgenic plants expressing the HDZhdip gene ATHB13. Plant Mol Biol **45**: 247–262

Harper AD, Bar-Peled M (2002) Biosynthesis of UDP-xylose: cloning and characterization of a novel Arabidopsis gene family, UXS, encoding soluble and putative membrane-bound UDP-glucuronic acid decarboxylase isoforms. Plant Physiol **130**: 2188–2198

Hepworth J, Lenhard M (2014) Regulation of plant lateral-organ growth by modulating cell number and size. Curr Opin Plant Biol **17**: 36–42

Hirsch S, Oldroyd GE (2009) GRAS-domain transcription factors that regulate plant development. Plant Signal Behav **4**: 698–700

Horiguchi G, Kim GT, Tsukaya H (2005) The transcription factor AtGRF5 and the transcription coactivator AN3 regulate cell proliferation in leaf primordia of Arabidopsis thaliana. Plant J **43**: 68–78

Horiguchi G, Van Lijsebettens M, Candela H, Micol JL, Tsukaya H (2012) Ribosomes and translation in plant developmental control. Plant Sci **191-192**: 24–34

Huang M, Slewinski TL, Baker RF, Janick-Buckner D, Buckner B, Johal GS, Braun DM (2009) Camouflage patterning in maize leaves results from a defect in porphobilinogen deaminase. Mol Plant **2**: 773–789

Ishida S, Takabayashi A, Ishikawa N, Hano Y, Endo T, Sato F (2009) A novel nuclear-encoded protein, NDH-dependent cyclic electron flow 5, is essential for the accumulation of chloroplast NAD(P)H dehydrogenase complexes. Plant Cell Physiol **50**: 383–393

Ito T, Kim GT, Shinozaki K (2000) Disruption of an Arabidopsis cytoplasmic ribosomal protein S13-homologous gene by transposon-mediated mutagenesis causes aberrant growth and development. Plant J **22**: 257–264

Juntawong P, Sorenson R, Bailey-Serres J (2013) Cold shock protein 1 chaperones mRNAs during translation in Arabidopsis thaliana. Plant J **74**: 1016–1028

Kärkönen A, Murigneux A, Martinant JP, Pepey E, Tatout C, Dudley BJ, Fry SC (2005) UDP-glucose dehydrogenases of maize: a role in cell wall pentose biosynthesis. Biochem J **391**: 409–415

Kazama T, Ichihashi Y, Murata S, Tsukaya H (2010) The mechanism of cell cycle arrest front progression explained by a KLUH/CYP78A5-dependent mobile growth factor for developing leaves of Arabidopsis thaliana. Plant Cell Physiol **51**: 1046–1054

Kim JH, Choi D, Kende H (2003) The AtGRF family of putative transcription factors is involved in leaf and cotyledon growth in Arabidopsis. Plant J **36**: 94–104

Kim JH, Kende H (2004) A transcriptional coactivator, AtGIF1, is involved in regulating leaf growth and morphology in Arabidopsis. Proc Natl Acad Sci USA **101**: 13374–13379

Kover PX, Valdar W, Trakalo J, Scarcelli N, Ehrenreich IM, Purugganan MD, Durrant C, Mott R (2009) A Multiparent Advanced Generation Inter-Cross to fine-map quantitative traits in Arabidopsis thaliana. PLoS Genet **5**: e1000551

Ku LX, Zhang J, Guo SL, Liu HY, Zhao RF, Chen YH (2012) Integrated multiple population analysis of leaf architecture traits in maize (Zea mays L.). J Exp Bot **63**: 261–274

Ku LX, Zhao WM, Zhang J, Wu LC, Wang CL, Wang PA, Zhang WQ, Chen YH (2010) Quantitative trait loci mapping of leaf angle and leaf orientation value in maize (Zea mays L.). Theor Appl Genet **121**: 951–959

Kumpf R, Thorstensen T, Rahman MA, Heyman J, Nenseth HZ, Lammens T, Herrmann U, Swarup R, Veiseth SV, Emberland G, et al (2014) The ASH1-RELATED3 SET-domain protein controls cell division competence of the meristem and the quiescent center of the Arabidopsis primary root. Plant Physiol **166**: 632–643

Larkin RM (2014) Influence of plastids on light signalling and development. Philos Trans R Soc Lond B Biol Sci **369**: 20130232

Lee BH, Ko JH, Lee S, Lee Y, Pak JH, Kim JH (2009) The Arabidopsis GRF-INTERACTING FACTOR gene family performs an overlapping function in determining organ size as well as multiple developmental properties. Plant Physiol **151**: 655–668

Lempiäinen H, Shore D (2009) Growth control and ribosome biogenesis. Curr Opin Cell Biol **21**: 855–863

Li P, Ponnala L, Gandotra N, Wang L, Si Y, Tausta SL, Kebrom TH, Provart N, Patel R, Myers CR, et al (2010) The developmental dynamics of the maize leaf transcriptome. Nat Genet **42**: 1060–1067

Li X, Zhu C, Yeh CT, Wu W, Takacs EM, Petsch KA, Tian F, Bai G, Buckler ES, Muehlbauer GJ, et al (2012) Genic and nongenic contributions to natural variation of quantitative traits in maize. Genome Res **22**: 2436–2444

Li Y, Zheng L, Corke F, Smith C, Bevan MW (2008) Control of final seed and organ size by the DA1 gene family in Arabidopsis thaliana. Genes Dev **22**: 1331–1336

Liepman AH, Cavalier DM (2012) The CELLULOSE SYNTHASE-LIKE A and CELLULOSE SYNTHASE-LIKE C families: recent advances and future perspectives. Front Plant Sci **3**: 109

Linkies A, Graeber K, Knight C, Leubner-Metzger G (2010) The evolution of seeds. New Phytol **186**: 817–831

Liu S, Melonek J, Boykin LM, Small I, Howell KA (2013a) PPR-SMRs: ancient proteins with enigmatic functions. RNA Biol **10**: 1501–1510

Liu WY, Chang YM, Chen SC, Lu CH, Wu YH, Lu MY, Chen DR, Shih AC, Sheue CR, Huang HC, et al (2013b) Anatomical and transcriptional

dynamics of maize embryonic leaves during seed germination. Proc Natl Acad Sci USA 110: 3979–3984

Love MI, Huber W, Anders S (2014) Moderated estimation of fold change and dispersion for RNA-seq data with DESeq2. Genome Biol 15: 550

Magnard JL, Heckel T, Massonneau A, Wisniewski JP, Cordelier S, Lassagne H, Perez P, Dumas C, Rogowsky PM (2004) Morphogenesis of maize embryos requires ZmPRPL35-1 encoding a plastid ribosomal protein. Plant Physiol 134: 649–663

Majeran W, Friso G, Ponnala L, Connolly B, Huang M, Reidel E, Zhang C, Asakura Y, Bhuiyan NH, Sun Q, et al (2010) Structural and metabolic transitions of C4 leaf development and differentiation defined by microscopy and quantitative proteomics in maize. Plant Cell 22: 3509–3542

Mansoori N, Timmers J, Desprez T, Alvim-Kamei CL, Dees DC, Vincken JP, Visser RG, Höfte H, Vernhettes S, Trindade LM (2014) KORRIGAN1 interacts specifically with integral components of the cellulose synthase machinery. PLoS ONE 9: e112387

Marino R, Ponnaiah M, Krajewski P, Frova C, Gianfranceschi L, Pè ME, Sari-Gorla M (2009) Addressing drought tolerance in maize by transcriptional profiling and mapping. Mol Genet Genomics 281: 163–179

Moon J, Candela H, Hake S (2013) The liguleless narrow mutation affects proximal-distal signaling and leaf growth. Development 140: 405–412

Morgante M, De Paoli E, Radovic S (2007) Transposable elements and the plant pan-genomes. Curr Opin Plant Biol 10: 149–155

Nelissen H, Eeckhout D, Demuynck K, Persiau G, Walton A, van Bel M, Vervoort M, Candaele J, De Block J, Aesaert S, et al (2015) Dynamic changes in ANGUSTIFOLIA3 complex composition reveal a growth regulatory mechanism in the maize leaf. Plant Cell 27: 1605–1619

Nelissen H, Rymen B, Jikumaru Y, Demuynck K, Van Lijsebettens M, Kamiya Y, Inzé D, Beemster GT (2012) A local maximum in gibberellin levels regulates maize leaf growth by spatial control of cell division. Curr Biol 22: 1183–1187

Niklas KJ (1994) Plant Allometry, the Scaling of Form and Process. University of Chicago Press, Chicago

Ohashi-Ito K, Bergmann DC (2007) Regulation of the Arabidopsis root vascular initial population by LONESOME HIGHWAY. Development 134: 2959–2968

Ori N, Cohen AR, Etzioni A, Brand A, Yanai O, Shleizer S, Menda N, Amsellem Z, Efroni I, Pekker I, et al (2007) Regulation of LANCEOLATE by miR319 is required for compound-leaf development in tomato. Nat Genet 39: 787–791

Palmieri L, Santoro A, Carrari F, Blanco E, Nunes-Nesi A, Arrigoni R, Genchi F, Fernie AR, Palmieri F (2008) Identification and characterization of ADNT1, a novel mitochondrial adenine nucleotide transporter from Arabidopsis. Plant Physiol 148: 1797–1808

Park YW, Tominaga R, Sugiyama J, Furuta Y, Tanimoto E, Samejima M, Sakai F, Hayashi T (2003) Enhancement of growth by expression of poplar cellulase in Arabidopsis thaliana. Plant J 33: 1099–1106

Pauly M, Qin Q, Greene H, Albersheim P, Darvill A, York WS (2001) Changes in the structure of xyloglucan during cell elongation. Planta 212: 842–850

Pelleschi S, Leonardi A, Rocher JP, Cornic G, De Vienne D, Thevenot C, Prioul JL (2006) Analysis of the relationships between growth, photosynthesis and carbohydrate metabolism using quantitative trait loci (QTLs) in young maize plants subjected to water deprivation. Mol Breed 17: 21–39

Peng M, Cui Y, Bi YM, Rothstein SJ (2006) AtMBD9: a protein with a methyl-CpG-binding domain regulates flowering time and shoot branching in Arabidopsis. Plant J 46: 282–296

Pérez-Pérez JM, Esteve-Bruna D, Micol JL (2010) QTL analysis of leaf architecture. J Plant Res 123: 15–23

Perry RP (2007) Balanced production of ribosomal proteins. Gene 401: 1–3

Persson S, Paredez A, Carroll A, Palsdottir H, Doblin M, Poindexter P, Khitrov N, Auer M, Somerville CR (2007) Genetic evidence for three unique components in primary cell-wall cellulose synthase complexes in Arabidopsis. Proc Natl Acad Sci USA 104: 15566–15571

Pfalz J, Liere K, Kandlbinder A, Dietz KJ, Oelmüller R (2006) pTAC2, -6, and -12 are components of the transcriptionally active plastid chromosome that are required for plastid gene expression. Plant Cell 18: 176–197

Pick TR, Bräutigam A, Schlüter U, Denton AK, Colmsee C, Scholz U, Fahnenstich H, Pieruschka R, Rascher U, Sonnewald U, et al (2011) Systems analysis of a maize leaf developmental gradient redefines the current C4 model and provides candidates for regulation. Plant Cell 23: 4208–4220

Piques M, Schulze WX, Höhne M, Usadel B, Gibon Y, Rohwer J, Stitt M (2009) Ribosome and transcript copy numbers, polysome occupancy and enzyme dynamics in Arabidopsis. Mol Syst Biol 5: 314

Poethig RS (1984) Cellular parameters of leaf morphogenesis in maize and tobacco. In RA White, WC Dickison, eds, Contemporary Problems in Plant Anatomy. Academic Press, New York, pp 235–259

Quesada V, Sarmiento-Mañús R, González-Bayón R, Hricová A, Ponce MR, Micol JL (2013) PORPHOBILINOGEN DEAMINASE deficiency alters vegetative and reproductive development and causes lesions in Arabidopsis. PLoS ONE 8: e53378

Rau A, Gallopin M, Celeux G, Jaffrézic F (2013) Data-based filtering for replicated high-throughput transcriptome sequencing experiments. Bioinformatics 29: 2146–2152

Rautengarten C, Ebert B, Herter T, Petzold CJ, Ishii T, Mukhopadhyay A, Usadel B, Scheller HV (2011) The interconversion of UDP-arabinopyranose and UDP-arabinofuranose is indispensable for plant development in Arabidopsis. Plant Cell 23: 1373–1390

Reboul R, Geserick C, Pabst M, Frey B, Wittmann D, Lütz-Meindl U, Léonard R, Tenhaken R (2011) Down-regulation of UDP-glucuronic acid biosynthesis leads to swollen plant cell walls and severe developmental defects associated with changes in pectic polysaccharides. J Biol Chem 286: 39982–39992

Ren B, Liang Y, Deng Y, Chen Q, Zhang J, Yang X, Zuo J (2009) Genome-wide comparative analysis of type-A Arabidopsis response regulator genes by overexpression studies reveals their diverse roles and regulatory mechanisms in cytokinin signaling. Cell Res 19: 1178–1190

Richter R, Behringer C, Müller IK, Schwechheimer C (2010) The GATA-type transcription factors GNC and GNL/CGA1 repress gibberellin signaling downstream from DELLA proteins and PHYTOCHROME-INTERACTING FACTORS. Genes Dev 24: 2093–2104

Richter R, Behringer C, Zourelidou M, Schwechheimer C (2013) Convergence of auxin and gibberellin signaling on the regulation of the GATA transcription factors GNC and GNL in Arabidopsis thaliana. Proc Natl Acad Sci USA 110: 13192–13197

Roberts AW, Frost AO, Roberts EM, Haigler CH (2004) Roles of microtubules and cellulose microfibril assembly in the localization of secondary-cell-wall deposition in developing tracheary elements. Protoplasma 224: 217–229

Rochange SF, McQueen-Mason SJ (2000) Expression of a heterologous expansin in transgenic tomato plants. Planta 211: 583–586

Romani I, Tadini L, Rossi F, Masiero S, Pribil M, Jahns P, Kater M, Leister D, Pesaresi P (2012) Versatile roles of Arabidopsis plastid ribosomal proteins in plant growth and development. Plant J 72: 922–934

Rymen B, Fiorani F, Kartal F, Vandepoele K, Inzé D, Beemster GT (2007) Cold nights impair leaf growth and cell cycle progression in maize through transcriptional changes of cell cycle genes. Plant Physiol 143: 1429–1438

Saeed AI, Sharov V, White J, Li J, Liang W, Bhagabati N, Braisted J, Klapa M, Currier T, Thiagarajan M, et al (2003) TM4: a free, open-source system for microarray data management and analysis. Biotechniques 34: 374–378

Sato S, Kato T, Kakegawa K, Ishii T, Liu YG, Awano T, Takabe K, Nishiyama Y, Kuga S, Sato S, et al (2001) Role of the putative membrane-bound endo-1,4-beta-glucanase KORRIGAN in cell elongation and cellulose synthesis in Arabidopsis thaliana. Plant Cell Physiol 42: 251–263

Shannon P, Markiel A, Ozier O, Baliga NS, Wang JT, Ramage D, Amin N, Schwikowski B, Ideker T (2003) Cytoscape: a software environment for integrated models of biomolecular interaction networks. Genome Res 13: 2498–2504

Sloan J, Backhaus A, Malinowski R, McQueen-Mason S, Fleming AJ (2009) Phased control of expansin activity during leaf development identifies a sensitivity window for expansin-mediated induction of leaf growth. Plant Physiol 151: 1844–1854

Sreeramulu S, Mostizky Y, Sunitha S, Shani E, Nahum H, Salomon D, Hayun LB, Gruetter C, Rauh D, Ori N, et al (2013) BSKs are partially redundant positive regulators of brassinosteroid signaling in Arabidopsis. Plant J 74: 905–919

Strand A, Asami T, Alonso J, Ecker JR, Chory J (2003) Chloroplast to nucleus communication triggered by accumulation of Mg-protoporphyrinIX. Nature 421: 79–83

Sun CW, Huang YC, Chang HY (2009) CIA2 coordinately up-regulates protein import and synthesis in leaf chloroplasts. Plant Physiol **150:** 879–888

Sylvester AW, Cande WZ, Freeling M (1990) Division and differentiation during normal and liguleless-1 maize leaf development. Development **110:** 985–1000

Tameshige T, Fujita H, Watanabe K, Toyokura K, Kondo M, Tatematsu K, Matsumoto N, Tsugeki R, Kawaguchi M, Nishimura M, et al (2013) Pattern dynamics in adaxial-abaxial specific gene expression are modulated by a plastid retrograde signal during Arabidopsis thaliana leaf development. PLoS Genet **9:** e1003655

Terry MJ, Smith AG (2013) A model for tetrapyrrole synthesis as the primary mechanism for plastid-to-nucleus signaling during chloroplast biogenesis. Front Plant Sci **4:** 14

Thimm O, Bläsing O, Gibon Y, Nagel A, Meyer S, Krüger P, Selbig J, Müller LA, Rhee SY, Stitt M (2004) MAPMAN: a user-driven tool to display genomics data sets onto diagrams of metabolic pathways and other biological processes. Plant J **37:** 914–939

Tian F, Bradbury PJ, Brown PJ, Hung H, Sun Q, Flint-Garcia S, Rocheford TR, McMullen MD, Holland JB, Buckler ES (2011) Genome-wide association study of leaf architecture in the maize nested association mapping population. Nat Genet **43:** 159–162

Tiller N, Bock R (2014) The translational apparatus of plastids and its role in plant development. Mol Plant **7:** 1105–1120

Tiller N, Weingartner M, Thiele W, Maximova E, Schöttler MA, Bock R (2012) The plastid-specific ribosomal proteins of Arabidopsis thaliana can be divided into non-essential proteins and genuine ribosomal proteins. Plant J **69:** 302–316

Veiseth SV, Rahman MA, Yap KL, Fischer A, Egge-Jacobsen W, Reuter G, Zhou MM, Aalen RB, Thorstensen T (2011) The SUVR4 histone lysine methyltransferase binds ubiquitin and converts H3K9me1 to H3K9me3 on transposon chromatin in Arabidopsis. PLoS Genet **7:** e1001325

Vercruyssen L, Verkest A, Gonzalez N, Heyndrickx KS, Eeckhout D, Han SK, Jégu T, Archacki R, Van Leene J, Andriankaja M, et al (2014) ANGUSTIFOLIA3 binds to SWI/SNF chromatin remodeling complexes to regulate transcription during *Arabidopsis* leaf development. Plant Cell **26:** 210–229

Voorend W, Lootens P, Nelissen H, Roldán-Ruiz I, Inzé D, Muylle H (2014) LEAF-E: a tool to analyze grass leaf growth using function fitting. Plant Methods **10:** 37

Wallace JG, Larsson SJ, Buckler ES (2014) Entering the second century of maize quantitative genetics. Heredity (Edinb) **112:** 30–38

Walsh J, Waters CA, Freeling M (1998) The maize gene liguleless2 encodes a basic leucine zipper protein involved in the establishment of the leaf blade-sheath boundary. Genes Dev **12:** 208–218

Wang J, Li M, Chen J, Pan Y (2011) A fast hierarchical clustering algorithm for functional modules discovery in protein interaction networks. IEEE/ACM Trans Comput Biol Bioinform **8:** 607–620

Wang L, Czedik-Eysenberg A, Mertz RA, Si Y, Tohge T, Nunes-Nesi A, Arrivault S, Dedow LK, Bryant DW, Zhou W, et al (2014) Comparative analyses of C₄ and C₃ photosynthesis in developing leaves of maize and rice. Nat Biotechnol **32:** 1158–1165

Wang P, Kelly S, Fouracre JP, Langdale JA (2013) Genome-wide transcript analysis of early maize leaf development reveals gene cohorts associated with the differentiation of C4 Kranz anatomy. Plant J **75:** 656–670

Weigel D (2012) Natural variation in Arabidopsis: from molecular genetics to ecological genomics. Plant Physiol **158:** 2–22

Wu G, Poethig RS (2006) Temporal regulation of shoot development in Arabidopsis thaliana by miR156 and its target SPL3. Development **133:** 3539–3547

Wu TD, Nacu S (2010) Fast and SNP-tolerant detection of complex variants and splicing in short reads. Bioinformatics **26:** 873–881

Yin T, Pan G, Liu H, Wu J, Li Y, Zhao Z, Fu T, Zhou Y (2012) The chloroplast ribosomal protein L21 gene is essential for plastid development and embryogenesis in Arabidopsis. Planta **235:** 907–921

Yu CP, Chen SC, Chang YM, Liu WY, Lin HH, Lin JJ, Chen HJ, Lu YJ, Wu YH, Lu MY, et al (2015) Transcriptome dynamics of developing maize leaves and genomewide prediction of cis elements and their cognate transcription factors. Proc Natl Acad Sci USA **112:** E2477–E2486

Zemach A, Grafi G (2007) Methyl-CpG-binding domain proteins in plants: interpreters of DNA methylation. Trends Plant Sci **12:** 80–85

Zhang LY, Bai MY, Wu J, Zhu JY, Wang H, Zhang Z, Wang W, Sun Y, Zhao J, Sun X, et al (2009) Antagonistic HLH/bHLH transcription factors mediate brassinosteroid regulation of cell elongation and plant development in rice and *Arabidopsis*. Plant Cell **21:** 3767–3780

Zilberman D, Cao X, Johansen LK, Xie Z, Carrington JC, Jacobsen SE (2004) Role of Arabidopsis ARGONAUTE4 in RNA-directed DNA methylation triggered by inverted repeats. Curr Biol **14:** 1214–1220